University of South Florida
Scholar Commons

Graduate Theses and Dissertations | Graduate School

November 2017

Enhancement of Two Passive Decentralized Biological Nitrogen Removal Systems

Justine L. Stocks
University of South Florida, stocksj@mail.usf.edu

Follow this and additional works at: http://scholarcommons.usf.edu/etd

Part of the Environmental Engineering Commons

Scholar Commons Citation

Stocks, Justine L., "Enhancement of Two Passive Decentralized Biological Nitrogen Removal Systems" (2017). *Graduate Theses and Dissertations.*
http://scholarcommons.usf.edu/etd/7093

This Thesis is brought to you for free and open access by the Graduate School at Scholar Commons. It has been accepted for inclusion in Graduate Theses and Dissertations by an authorized administrator of Scholar Commons. For more information, please contact scholarcommons@usf.edu.

Enhancement of Two Passive Decentralized Biological Nitrogen Removal Systems

by

Justine L. Stocks

A thesis submitted in partial fulfillment
of the requirements for the degree of
Master of Science in Engineering Science
Department of Civil and Environmental Engineering
College of Engineering
University of South Florida

Major Professor: Sarina J. Ergas, Ph.D.
Kebreab Ghebremichael, Ph.D.
James Mihelcic, Ph.D.
Damann Anderson, M.S.

Date of Approval:
October 26, 2017

Keywords: Pilot Study, Household Wastewater Treatment, Ion Exchange, Pyrite Oxidizing Denitrification, Oyster Shells, SEM-EDS

Copyright © 2017, Justine L. Stocks

DEDICATION

To my family, friends, and future husband. I love y'all.

ACKNOWLEDGMENTS

The utmost gratitude goes to my major professor, Sarina J. Ergas, for her patience and guidance on these projects and Shuang Tong and Laura Rodriguez-Gonzalez for their mentorship. Also to Josefin Hirst and Damann Anderson for their expert advice which was crucial for the implementation of the Pilot Project and Dr. Kebreab Ghebremichael and Dr. James Mihelcic for their guidance and participation in this project. Analytical work for this project was made possible by Nadezhda Zalivina, the lab IC guru. Zachary Carroll provided much support during the construction of the pilot and made the AutoCad drawing of the system. Special thanks to Northwest Regional Water Reclamation Facility in Citrus Park, Florida and their staff for their assistance during the construction and operation of the Pilot system, especially during their major plant expansion. I would also like to thank the rest of my lab group for their assistance in the construction of the pilot and wish Amulya Miryala and Michelle Henderson luck in their continued work on the system. I would also like to acknowledge the Richard and Stessel Mern Memorial Scholarship for financial support for tuition, research and stipends. A big thank you goes to my fiancé Kevin, who supported me throughout this journey. And last but definitely not least, I would like to thank my grandmother, Ruth, whose generosity and hospitality made this goal possible.

This publication was made possible by USEPA grant 83556901. Its contents are solely the responsibility of the grantee and do not necessarily represent the official views of the USEPA. Further, USEPA does not endorse the purchase of any commercial products or services mentioned in this publication.

TABLE OF CONTENTS

LIST OF TABLES iii

LIST OF FIGURES iv

ABSTRACT v

CHAPTER 1: INTRODUCTION 1

CHAPTER 2: STARTUP OF A PILOT SCALE PASSIVE NITROGEN REDUCTION SYSTEM 5

- 2.1 Introduction 5
- 2.2 Literature Review 10
  - 2.2.1 Biological Nutrient Removal 10
  - 2.2.2 Adsorption and Ion Exchange 12
  - 2.2.3 Recirculation 15
  - 2.2.4 Passive Nitrogen Reduction Systems 16
  - 2.2.5 Oyster Shell as an Alkalinity Source 19
  - 2.2.6 Hybrid Adsorption and Biological Treatment Systems 19
- 2.3 Materials and Methods 21
  - 2.3.1 System Configuration and Influent Feeding 21
  - 2.3.2 Media Materials 21
  - 2.3.3 System Components 22
  - 2.3.4 Startup 22
  - 2.3.5 Operation 22
  - 2.3.6 Sample Analysis 23
  - 2.3.7 Statistical Analysis 24
- 2.4 Results and Discussion 28
  - 2.4.1 Nitrification Stage 1 Performance 28
  - 2.4.2 Denitrification Stage 2 Performance 30
  - 2.4.3 Overall System Performance 31
- 2.5 Conclusions 39

CHAPTER 3: ANALYSIS OF BIOFILM DISTRIBUTIONS IN PARTICULATE PYRITE AUTOTROPHIC DENITRIFICATION PROCESS WITH AND WITHOUT OYSTER SHELLS 41

3.1 Introduction 41
3.2 Literature Review 43
3.2.1 Pyrite Oxidizing Denitrification 43
3.2.2 Particulate Pyrite Autotrophic Denitrification 45
3.2.3 Oyster Shell as a Biofilm Carrier 46
3.3 Materials and Methods 46
3.3.1 Sample Collection 46
3.3.2 SEM-EDS 47
3.3.3 Statistical Analysis 48
3.4 Results and Discussion 48
3.4.1 SEM-EDS Results 48
3.4.2 SEM Images to Observe Surface Characteristics and Biofilm Distributions 50
3.5 Conclusions 54

CHAPTER 4: CONCLUSIONS AND RECOMMENDATIONS 55

REFERENCES 57

APPENDIX A LIST OF ACRONYMS 62

APPENDIX B SUPPLEMENTARY DATA FOR CHAPTER 2 64

APPENDIX C DESIGN SPECIFICATIONS AND PHOTOS OF THE PILOT SYSTEM 70

APPENDIX D COPYRIGHT PERMISSION 73

LIST OF TABLES

Table 2.1	TN results from Anderson et. al. (1998) in mg L^{-1} as N.	17
Table 2.2	Media characteristics and composition of each system for nitrification stage 1 and denitrification stage 2.	24
Table 2.3	Pilot system component descriptions and manufacturers.	25
Table 2.4	HRTs of each stage throughout the study calculated by Empty Bed Contact Time (EBCT).	28
Table 2.5	Average N species results for influent, R-1 and FF-1 biofilters for the duration of the study.	33
Table 2.6	Average water quality results for influent, R-1 , R-2, FF-1 and FF-2 biofilters from day 17-day 59 of the study.	38
Table 2.7	Total TIN removal efficiencies from influent to effluent of R-1 and FF-1 and overall TIN removal after denitrification stage 2 (R-2 and FF-2) for the duration of the study.	39
Table 3.1	Description of column study comparing P+S+OS and P+S adapted from Tong et al. (2017).	43
Table 3.2	Energy Dispersive X-Ray Spectroscopy data (averages) in atomic percentage units for pyrite and oyster shell samples from before the experiment and taken from port 1 (near inlet) and port 5 (near outlet) n = 2.	51
Table B.1	Daily water quality data for the influent of R and FF.	64
Table B.2	Daily water quality data for R-1.	65
Table B.3	Daily water quality data for R-2.	66
Table B.4	Daily water quality data for FF-1.	67
Table B.5	Daily water quality data for FF-2.	68

LIST OF FIGURES

Figure 2.1	Schematic of the two side by side systems (R and FF) and septic tank.	25
Figure 2.2	Dosing schedule for pilot system (FF-system and R-system) at the 35.5 gallon d^{-1} flow rate.	27
Figure 2.3	Daily variations of a) NH_4^+, b) Na^+, c) NO_2^-, d) NO_3, and e) TIN for influent, R-1 and FF-1.	32
Figure 2.4	Daily variations of a) NH_4^+-N, b) TIN, c)NO_2^--N for influent, R-2 and FF-2 and d) NO_3^--N for influent, R-1, FF-1, R-2 and FF-2.	34
Figure 2.5	Average sCOD for influent, stage 1 and stage 2 for both systems for the duration of the study.	35
Figure 2.6	Daily variations for sCOD for influent and effluent of stage 2 for each system: a) R-1 and R-2 and b) FF-1 and FF-2.	36
Figure 2.7	Sulfate (as SO_4^{2-}-S) daily variations for a) influent, FF-1, and FF-2 and b) influent, R-1 and R-2 from day 16-day 58 of the study.	37
Figure 3.1	Image of one column from the experiment with vertical ports labeled.	47
Figure 3.2	SEM images of particulate pyrite, quartz sand and oyster shell before (a, b and c) and after the experiment from ports 1 (influent) and 5 (effluent) from the P+ S column (d, e, f and g) and ports 1 and 5 from the P+S+OS column (h, i, j, k, l and m).	52
Figure 3.3	Protein results from a) attached biomass and b) pore water from Tong et al. (2017b).	53
Figure C.1	Complete sketch of pilot system from recirculation (R) side.	70
Figure C.2	Image taken from the forward flow (FF) side of the pilot system, showing (left to right) stage 2, stage 1 and the septic tank.	71
Figure C.3	Image taken of the R side of the pilot system showing (left to right) stage 2, recirculation pump tank, stage 1, and recirculation tank.	72

ABSTRACT

This research evaluates two different Biological Nitrogen Removal (BNR) systems for enhanced nitrogen removal in decentralized wastewater treatment. The first study evaluated the performance of Hybrid Adsorption and Biological Treatment Systems (HABiTS) at the pilot scale with and without stage 1 effluent recirculation. HABiTS is a system developed at the bench scale in our laboratory and was designed for enhanced BNR under transient loading conditions. It consists of two stages; an ion exchange (IX) onto clinoptilolite media coupled with biological nitrification in the aerobic nitrification stage 1 and a Tire-Sulfur Adsorption Denitrification (T-SHAD) system in the anoxic denitrification stage 2. The T-SHAD process incorporates NO_3^- adsorption onto tire chips and Sulfur Oxidizing Denitrification (SOD) using elemental sulfur as the electron donor for NO_3^- reduction. Previous bench scale studies evaluated HABiTS performance under transient loadings and found significantly higher removal of nitrogen with the incorporation of adsorptive media in stage 1 and 2 compared with controls (80% compared to 73%) under transient loading conditions.

In this study, we hypothesize that a HABiTS system with effluent recirculation in nitrification stage 1 may enhance nitrogen removal performance compared to that without recirculation. The following were the expected advantages of Stage 1 effluent recirculation for enhanced nitrogen removal:

1) Pre-denitrification driven by the mixture of nitrified effluent from stage 1 with high concentrations of biochemical oxygen demand (BOD) septic tank effluent.

2) Moisture maintenance in stage 1 for enhanced biofilm growth.

3) Increased mass transfer of substrates to the biofilm in stage 1.

4) Decreased ratio of BOD to Total Kjeldahl Nitrogen (TKN) in the influent of stage 1.

Two side-by-side systems were run with the same media composition and fed by the same septic tank. One had a nitrification stage 1 effluent recirculation component (R-system), which operated at a 7:1 stage 1 effluent recirculation ratio for the first 49 days of the study and at 3:1 beginning on day 50 and one was operated under forward flow only conditions (FF-system). The R system removed a higher percentage of TIN (35.4%) in nitrification stage 1 compared to FF (28.8%) and had an overall TIN removal efficiency of 88.8% compared to 54.6% in FF system. As complete denitrification was observed in stage 2 throughout the study, overall removal was dependent on nitrification efficiency, and R-1 had a significantly higher NH_4^+ removal (87%) compared to FF-1 (70%). Alkalinity concentrations remained constant from stage 1 to stage 2, indicating that some heterotrophic denitrification was occurring along with SOD, as high amounts of sCOD leached from the tire chips in the beginning of the study, reaching sCOD concentrations of 120-160 mg L^{-1} then decreasing after day 10 of operation of stage 2. Sulfate concentrations from stage 2 for each side were low until the last 10 days of the study, with an average of 16.43 ± 11.36 mg L^{-1} SO_4^{2-}-S from R-2 and an average of 16.80 ± 7.98 SO_4^{2-}-S for FF-2 for the duration of the study, however at the end of the study when forward flow rates increased, SO_4^{2-}-S concentrations increased to 32 mg L^{-1} for R-2 and 40 mg L^{-1} for FF-2. Similar performance was observed in the FF system as the bench scale reactor tests.

The second part of the research focused on the findings from a study of a Particulate Pyrite Autotrophic Denitrification (PPAD) process that uses pyrite as the electron donor and nitrate as the terminal electron acceptor in upflow packed bed bioreactors. The advantages of using pyrite

as an electron donor for denitrification include less sulfate production and lower alkalinity requirements compared with SOD. The low alkalinity consumption of the PPAD process led to comparison of PPAD performance with and without oyster shell addition. Two columns were operated side-by-side, one packed with pyrite and sand only (P+S), while another one was packed with pyrite, sand and oyster shell (P+S+OS). Sand was used as a nonreactive biofilm carrier in the columns. My contribution to this research was to carry out Scanning Electron Microscopy-Energy-Dispersive X-Ray Spectroscopy (SEM-EDS) analysis to support the hypothesis that oyster shell contributes to nitrogen removal because it has a high capacity for biofilm attachment. SEM analysis showed that oyster shell has a rough surface, supported by its high specific surface area, and that there was more biofilm attached to oyster shell than pyrite or sand in the influent to the column. EDS results showed a decrease in atomic percentages for pyrite sulfur in the effluent of both columns (59.91% ± 0.10% to 53.94% ± 0.37% in P+S+OS column and to 57.61% ± 4.21% in P+S column). This finding indicated that sulfur was oxidized more than iron and/or the accumulation of iron species on the pyrite surface and supports the coupling of NO_3^- reduction with pyrite oxidation.

CHAPTER 1: INTRODUCTION

Nitrogen pollution is a major concern in many parts of the world. Excess nitrogen inputs into nitrogen-limited environments such as estuaries and other coastal environments can cause toxic algal blooms, which result in hypoxic zones and fish die-offs. Inorganic nitrogen enters aquatic environments in the form of ammonium (NH_4^+), nitrite (NO_2^-) or nitrate (NO_3^-). The Maximum Contaminant Levels (MCL) set by the United States Environmental Protection Agency (USEPA) for NO_3^--N and NO_2^--N for drinking water are 10 mg L^{-1} and 1 mg L^{-1}, respectively (USEPA, 2017). When humans consume drinking water with excess concentrations of NO_3^- or NO_2^-, a condition known as methemoglobinemia (blue baby syndrome) can occur, which is especially dangerous to infants and can also effect livestock (Wright et al., 1999).

A major source of inorganic nitrogen to the aquatic environment is poorly treated wastewater, with Onsite Wastewater Treatment Systems (OWTS) making up a large portion of this nitrogen input (USEPA 2002). Conventional OWTS consist of a septic tank, which removes most of the solids via settling and a drainfield in which the effluent from the septic tank is dispersed and secondary treatment, including cBOD, TSS, bacterial reductions, nitrification and some denitrification (25-50% TN removal) and phosphorus removal can occur if designed properly. However, high rates of failure due to improper maintenance, siting, and poor enforcement of regulations for effluent quality for OWTS contribute to the high levels of inorganic nitrogen that they release into the environment (USEPA, 2002).

A large majority of the Total Inorganic Nitrogen (TIN) in septic tank effluent is in the form of NH_4^+ (98.6% from the septic tank in this study). This is because anaerobic conditions persist

within the septic tank, therefore only settling of solids and some ammonification can occur, but not nitrification, which requires aerobic conditions (Rittmann and McCarty, 2001). Two-stage Passive Nitrogen Reducing Systems (PNRS) incorporating Biological Nitrogen Removal (BNR) processes using an aerobic nitrification stage 1 followed by an anoxic denitrification stage 2 with a reactive medium have the potential to remove a large portion of nitrogen in the effluent of the septic tank and can intercept the septic tank and drainfield (Hazen and Sawyer, 2015); however, BNR processes alone are vulnerable to transient loadings characteristic of OWTS. As flows in OWTS are determined by human activities, they tend to fluctuate throughout the day. Since it is difficult for microbial populations to buffer these loads if they exceed microbial biodegradation capacity, the treatment efficiency of the system suffers (USEPA, 2002). Additionally, idle periods, which occur when people go on vacation, can cause die-offs of microbial populations due to the absence of substrate, which can also cause slow start up times afterwards.

Addressing this issue, Hazen and Sawyer (2014) added ion exchange (IX) media clinoptilolite to the nitrification stage 1 filter media in 2-stage BNR PNRS pilot studies, followed by Sulfur Oxidizing Denitrification (SOD) and consistently achieved Total Kjeldahl Nitrogen (TKN) removals of over 95%. In full-scale field studies (Hazen and Sawyer, 2015), the highest total nitrogen (TN) removal efficiencies in nitrification stage 1 were achieved in the system using nitrification stage 1 effluent recirculation at a 3:1 recirculation ratio (FOSNRS, 2015). Rodriguez-Gonzalez (2017) developed a novel two-stage Passive Nitrogen Reducing (PNRS) system, called Hybrid Adsorption and Biological Treatment Systems (HABiTS). This system employs an aerobic nitrification stage 1 trickling filter with clinoptilolite for IX of NH_4^+ and expanded clay as a biofilm carrier. Denitrification stage 2 consists of a novel Tire-Sulfur Hybrid Adsorption Denitrification (T-SHAD) process with tire chips for adsorption of NO_3^- and the addition of some organic carbon

for mixotrophic denitrification, oyster shell as an alkalinity source, and elemental sulfur for autotrophic (SOD). Both stages employ IX to address the issue of transient loading and idle times in OWTS.

SOD is a highly-studied method for BNR. It is an autotrophic process in which elemental sulfur is used as the electron donor and CO_2 as the carbon source (Rittmann and McCarty, 2001). As elemental sulfur is non-toxic, water insoluble, stable under normal conditions, and readily available, much more attention has been paid to SOD of nitrate contaminated wastewater (Sahinkaya and Kilic, 2014). SOD has several advantages to heterotrophic denitrification, including less sludge yield and lower secondary organic pollution. It is an efficient denitrification process, as it can reach denitrification rates of up to 820 mg NO_3^--N L^{-1} d^{-1} (Tong et al., 2017a). However, disadvantages associated with SOD include high sulfate production and alkalinity consumption (Lee et al., 2011). The secondary standard for SO_4^{2-} for drinking water set by the USEPA is 250 mg L^{-1}.

An alternative to SOD is the use of pyrite as a solid-phase electron donor for denitrification. Tong et al. (2017a) developed a novel Particulate Pyrite Autotrophic Denitrification (PPAD) process for the treatment of nitrified wastewater and compared denitrification rates to those of SOD. Although a lower denitrification efficiency was observed in PPAD than SOD (39.7% and 99.9%, respectively), the denitrification efficiency of PPAD was similar to those observed in other studies for SOD (Sahinkaya & Durson, 2012; Smith, 2012). Furthermore, previous studies also demonstrated that higher denitrification efficiencies can be achieved by adding both sand and oyster shell to the columns, which have high surface areas, and thus provide increased area for biofilm attachment (Sengupta et al., 2007; Lai et al., 2000), leading to additional biological treatment. Tong et al. (2017b) compared PPAD columns with (P+S+OS) and without (P+S) oyster

shells to determine the effects of oyster shell on the treatment in the PPAD column. With the addition of 10% by volume organic substrate to the synthetic nitrified wastewater, P+S+OS exhibited a higher TIN removal efficiency (90%) than P+S (70%) and some nitrification was also observed in the P+S+OS column.

This thesis aims to build on the works by Rodriguez-Gonzalez (2017) and Tong et al. (2017a & 2017b) and further investigate the performance of HABiTS in a pilot-scale study. Two side-by-side systems with the same media compositions (R and FF systems) were fed screened raw wastewater from the Northwest Regional Water Reclamation Facility in Tampa, Florida. Media analysis on PPAD P+S and P+S+OS columns from Tong et al. (2017b) was also done to elucidate the role of oyster shell in the treatment in the system. More specifically, the main objectives of this research were to:

1) Investigate the startup of a pilot scale HABiTS system
2) Investigate the effect of nitrification stage 1 effluent recirculation at a 7:1 (day 1-49) and 3:1 (day 50 on) recirculation ratio on nitrogen removal in the HABiTS system
3) Elucidate the role of oyster shell in the nitrogen removal in the PPAD system.

This thesis is divided into three subsequent chapters: Chapter 2: Startup of a Pilot Scale Passive Nitrogen Reduction System, which covers the first two objectives, Chapter 3: Analysis of Biofilm Distributions in PPAD Process With and Without Oyster Shells, which covers the third objective, and Chapter 4, which presents overall conclusions and recommendations.

CHAPTER 2: STARTUP OF A PILOT SCALE PASSIVE NITROGEN REDUCTION SYSTEM

2.1 Introduction

Onsite Wastewater Treatment Systems (OWTS) treat about one third of the wastewater produced in the U.S. and failing systems represent the third largest contributor to ground water pollution due to inadequate maintenance or inappropriate siting or design (USEPA 2002). Lapointe et al. (1990) studied effects of inadequate OWTS on nutrient levels in groundwater and surface water around the Florida Keys, an area that is not ideal for secondary treatment in conventional OWTS, and utilized systems that were not up to code, such as cesspits. The study found a 5000-fold overall nutrient enrichment and a 400-fold enrichment of dissolved inorganic nitrogen (NH_4^++NO_3^-+NO_2^-) in areas contiguous to OWTS. Releases of nutrients into the environment cause problems such as eutrophication in surface waters, which leads to hypoxia, fish die offs and compromises to sea grass populations. As coastal waters are typically nitrogen-limited, these systems are especially vulnerable to eutrophication caused by anthropogenic nitrogen inputs. In a study by Bricker, et al. (2007), 78% of the studied estuarine areas were shown to be moderately to highly eutrophic as a result of human actions, some of which is discharge from failing OWTS.

Conventional OWTS consist of a septic tank for solids separation and some anaerobic primary treatment and a soil treatment unit, or drainfield, for nitrification, biological treatment, and pathogen removal, and denitrification in the lower drainfield, depending on quality of soil and/or bedrock. Although these systems are designed to remove 25-50% of total nitrogen (TN),

their rate of failure and improper maintenance or siting causes them to release nitrogen levels that exceed those required in nutrient sensitive environments (USEPA, 2002). As anaerobic conditions persist in the septic tank, almost all aqueous nitrogen from septic tanks is released in the form of ammonium (NH_4^+). The NH_4^+ is converted to nitrate (NO_3^-) in the upper drain field and depending on the depth and permeability of the subsurface under the drain field, some percentage can be removed via denitrification. Many areas that use OWTS, such as the Florida Keys, do not have suitable soils for construction of conventional OWTS, and must resort to alternative OWTS to provide adequate treatment. Under some soil conditions, little or no denitrification occurs. In this case, almost all the nitrogen leaving the OWTS enters the groundwater in the form of NO_3^-. Aside from causing environmental problems such as eutrophication, excess NO_3^- can also be toxic to humans, leading to methemoglobinemia, also known as blue baby syndrome in infants, which is a condition that leads to reduced oxygen in the blood (USEPA, 2017).

Connecting more homes to centralized treatment is one solution to the problem of nitrogen discharges from OWTS (Metropolitan St. Louis Sewer District, 2016). However, in rural areas or on islands with low population density, such as the Florida Keys, connecting to sewer lines is not feasible and onsite or decentralized treatment must be improved to maintain groundwater quality and reduce nutrient and pathogen inputs. Some newer systems, called Aerobic Treatment Units (ATUs) employ active aeration within the tank to promote nutrient and BOD (Biochemical Oxygen Demand) removal; however, these systems have high energy requirements and can be costly to maintain by the homeowner (USEPA, 2002). Passive nitrogen reduction systems (PNRS) have been tested at the laboratory, pilot scale and household, and have shown good removal of nitrogen with low energy requirement (Rodriguez-Gonzalez, 2017 & Hazen and Sawyer, 2014 & 2015). PNRS typically consist of a septic tank and secondary treatment units, which may include one or

more biofilters comprised of different types of media, treating the septic tank effluent before it is released to the drain field. Nutrient removal is accomplished using Biological Nitrogen Removal (BNR) processes.

BNR is a widely used and effective way to treat wastewater, due to its low maintenance and cost requirements compared with physical-chemical systems (USEPA, 2007). It is also the most common method for nitrogen removal, which utilizes microbial metabolism for nitrogen species transformation. As most of the nitrogen in septic tank effluent is in the form of ammonia (NH_4^+), it must first go through nitrification in the presence of oxygen, which occurs via aerobic oxidation of NH_4^+ ($NH_4^+ \rightarrow NO_2^- \rightarrow NO_3^-$), followed by denitrification in the absence of oxygen, or reduction of NO_3^- ($NO_3^- \rightarrow NO_2^- \rightarrow N_2(g)$) to be removed as dinitrogen gas. Hazen and Sawyer (2015) evaluated nitrogen removal performance in two-stage advanced PNRS, and reported mean Total Nitrogen (TN) removals from all systems ranging from 65-98%. Advanced treatment BNR systems fall under the "Alternative Systems" definition of OWTS in Florida (FDOH 2013). In areas with low topography like Florida, passive systems can be defined as systems using 1 pump or less as the only mechanical input and reactive media for denitrification (FDOH, 2013). Different media have also been examined for advanced treatment of onsite wastewater using PNRS, including but not limited to sand (Anderson et al., 1998), expanded clay (Hazen and Sawyer, 2015), crushed brick (Anderson et al., 1998), wood chips (reviewed in Lopez-Ponnada et al., 2017), clinoptilolite (Hazen and Sawyer, 2014 and Rodriguez-Gonzalez, 2017), tire chips (Krayzelova et al., 2015), pyrite (Torrento et al., 2010 and Pu et al., 2014) and sulfur (Hazen and Sawyer, 2015 and Krayzelova et al., 2014). Media such as sand and expanded clay are mainly used as biofilm carriers, clinoptilolite and tire chips are an adsorptive surface for NH_4^+ and NO_3^-, respectively, and wood chips, tire chips, pyrite and sulfur contribute substrate and electron donors for biological

denitrification (Anderson et al., 1998). Oyster shells are a slow-release alkalinity source and a good biofilm carrier that has also been used in PNRS (Sahinkaya et al., 2011; Tong et al., 2017b).

One issue with advanced OWTS with potentially detrimental effects on BNR processes is the transient loading that is characteristic of OWTS. Influent flow rates are typically transient, as they depend on daily human routines and activities (NSF 2013). This results in high loading rate periods during the morning, afternoon and evening, which introduces substrate in excess of microbial degradation capacity. This may result in a decrease in treatment efficiency of the systems. Additionally, microbial communities cannot withstand extended idle periods and the long startup after an idle period can impede performance of the system (Rodriguez-Gonzalez et al., 2017). Recent studies demonstrated that clinoptilolite, an ion exchange (IX) medium, has an affinity for NH_4^+ (Rodriguez-Gonzalez, 2017). A novel PNRS designed for onsite treatment called Hybrid Adsorption and Biological Treatment Systems (HABiTS) was developed by Rodriguez-Gonzalez (2017) and incorporates expanded clay and clinoptilolite for the nitrification stage 1. In bench scale studies comparing a column with expanded clay and clinoptilolite to a column with expanded clay only, the column with clinoptilolite achieved a NH_4^+ removal efficiency of 80%, compared to 73% in the control column. Average NH_4^+ concentrations were significantly lower in the HABiTS column throughout the study.

With respect to denitrification processes in OWTS, the high variability in loading rates, long idle periods and lack of regular maintenance presents a challenge for biological nitrogen removal in OWTS (Krayzelova et al., 2014). A Tire-Sulfur Hybrid Adsorption Denitrification (T-SHAD) process was developed that combines nitrate (NO_3^-) adsorption to scrap tire chips with Sulfur Oxidizing Denitrification (SOD). This allows the tire chips to adsorb NO_3^- when the influent loading exceeds the denitrification capacity of the biofilm and release it when NO_3^- loading rates

are low (e.g. at night) (Krayzelova et al., 2014). A recent study conducted by Krayzelova et al. (2014) on T-SHAD also revealed that scrap tires leach bioavailable organic carbon, with heterotrophic processes contributing to about 20% of the denitrification of the system. For the denitrification stage 2, the T-SHAD system for Sulfur Oxidizing Denitrification (SOD) is used.

In addition, nitrification stage 1 effluent recirculation has the potential to increase nitrogen removal by combining nitrified effluent from nitrification stage 1 with septic tank effluent, which has some bioavailable organic carbon, therefore promoting pre-denitrification. Hazen and Sawyer (2015) evaluated seven full-scale prototype PNRS systems and observed the highest nitrification stage 1 total nitrogen (TN) removal (61%) in the system that incorporated nitrification stage 1 effluent recirculation. This result was attributed to pre-denitrification. Other possible benefits of recirculation include maintaining moisture in nitrification stage 1 media during idle times, increased mass transfer through the nitrification stage 1 filter due to a higher flow rate, and decreasing soluble Chemical Oxygen Demand (sCOD) concentrations in nitrification stage 1 influent, which creates a better environment for the growth of nitrifiers by decreasing competition with heterotrophs (Rittmann and McCarty, 2015). To investigate the effect of recirculation, this study tested two side-by-side pilot-scale HABiTS systems, one with a 7:1 (day 1-49) then a 3:1 (day 50 on) recirculation ratio (R) and one with forward flow only (FF).

The overall goal of this research was to test HABiTS at the pilot scale and to assess the effects of recirculation on the nitrogen removal performance of the system. This system utilized a nitrification step composed of expanded clay, oyster shell, and clinoptilolite as an IX media and a denitrification step which is composed of a novel Tire-Sulfur Autotrophic Denitrification (T-SHAD) system (Krayzelova et al., 2014). Two side-by side systems were run with the same

influent feed, one with recirculation (R) and one without (FF), as shown in Figure 2.1. The main objectives of this study were to:

1) Investigate the startup of a pilot scale HABiTS system
2) Investigate the effect of nitrification stage 1 effluent recirculation at a 7:1 (day 1-49) and 3:1 (day 50 on) recirculation ratio on nitrogen removal in the HABiTS system

2.2 Literature Review

2.2.1 Biological Nutrient Removal

Biological Nitrogen Reduction (BNR) is commonly used to address the problem of nitrogen release from wastewater treatment systems. As the nitrogen species in domestic wastewater are mainly in the form of ammonium (NH_4^+) and organic nitrogen, biological processes must occur in 2 stages:

1) Nitrification

$$NH_4^+ + 1.815\ O_2 + 0.1304\ CO_2 \rightarrow$$
$$0.0261\ C_5H_7O_2N + 0.973\ NO_3^- + 0.921\ H_2O + 1.973\ H^+ \quad (1)$$

2) Denitrification using methanol (CH_3OH) as an electron donor

$$0.17\ CH_3OH + 0.16\ NO_3^- + 0.16\ H^+ \rightarrow$$
$$0.01\ C_5H_7O_2N + 0.38\ N_2 + 0.12\ CO_2 + 0.38\ H_2O \quad (2)$$

As nitrite (NO_2^-) is an intermediate product in these two reactions, it can be used as an indicator for these processes. The nitrification step involves chemoautotrophic bacteria that use ammonium and nitrite (NO_2^-) as the electron donor and oxygen as the terminal electron acceptor. An oxygen-rich environment and a consistent supply of ammonium needs to be maintained in this process. The oxygen demand of nitrification is 4.57 g O_2 for each g NH_4^+-N nitrified. Nitrification also consumes 7.05 g of alkalinity (as $CaCO_3$) g^{-1} NH_4^+-N oxidized. Competition with heterotrophs

(organisms using organic carbon as an electron donor) can impede the growth of nitrifiers due to their low biomass yield compared to heterotrophs, so low concentrations of organic carbon available for microorganisms, known as Carbonaceous Biochemical Oxygen Demand (cBOD) are ideal for nitrifiers. Total Kjeldahl Nitrogen (TKN) is the sum of NH_4^+ and organic nitrogen, which can be hydrolyzed to NH_4^+. Therefore, high TKN:BOD ratios are ideal in wastewater feeding biological nitrification processes.

The second step in BNR is denitrification. Equation 2 shows chemoheterotrophic denitrification using acetate, an organic carbon source, as the electron donor. In an anoxic environment, these organisms use nitrate as the terminal electron acceptor, reducing it to dinitrogen gas. If oxygen is present, they will use oxygen as the terminal electron acceptor, hence the designation "facultative". An electron donor can either be organic carbon released from a source such as wood chips or acetate (chemoheterotrophic) or an inorganic compound such as elemental sulfur, pyrite or hydrogen gas (chemoautotrophic). Chemoheterotrophic denitrification produce alkalinity (Equation 2), while chemoautotrophic denitrification consume alkalinity. Sulfur oxidizing denitrification (SOD) is a chemoautotrophic denitrification process. This process produces sulfate, as can be observed in the following stoichiometric equation (Sahinkaya et al., 2011):

$$55S^0 + 20\ CO_2 + 50NO_3^- + 38H_2O + 4NH_4^+ \rightarrow 4C_5H_7O_2N + 25N_2 + 55SO_4^{2-} + 64H^+ \quad (3)$$

This process removes NO_3^- via it's reduction to N_2 (gas). It produces 7.54 g SO_4^{2-} and consumes 4.57 g alkalinity (as $CaCO_3$) per gram of NO_3^--N removed. Mixotrophic metabolism can occur if both inorganic and organic electron donors are available. Chemoautotrophic metabolism has the advantages of 1) less sludge production and 2) no need for addition of an organic chemical. Chemoautotrophic denitrification processes consume alkalinity, as shown in Equation 3, so an

alkalinity source is needed to maintain an optimal pH (6-8) in the system (Rittman and McCarty, 2001).

2.2.2 Adsorption and Ion Exchange

Adsorption is a process in which a substance, called the adsorbate, in the liquid phase undergoes mass transfer and accumulation onto a solid, or the adsorbent. Adsorption can be carried out either by chemical reactions between the adsorbate and the adsorbent (chemisorption) or physical processes (physical adsorption). The most common type of adsorption in water/wastewater applications is physical adsorption. Mechanisms for physical adsorption include van der Waals forces and ion displacement, also known as ion exchange (IX) (Crittenden et al., 2012).

IX is a physical process in which ions in the aqueous phase are exchanged with ions in the solid phase. This process occurs on an ion exchanger with an opposite surface charge to that of the ions being exchanged. A common mineral used for cation exchange is natural zeolite. The selectivity of zeolites is determined by the unique pore structures built by their aluminosilicate matrix, which gives them specific sieving properties (Ames, 1960). Ames (1960) determined the order of affinity for cations on zeolites to be $Cs^{+}>Rb^{+}>K^{+}>NH_4^{+}>Ba^{2+}>Na^{+}>Ca^{2+}>Fe^{3+}>Mg^{2+}$. Equation 4 is a representation of IX on the surface of zeolite as adapted from Ames (1960) and Aponte-Morales (2015) where Z=Zeolite, or ion exchange media.

$$Z - Na_2 + \begin{bmatrix} Ca^{2+} \\ Mg^{2+} \\ 2NH_4{}^{+} \\ 2K^{+} \end{bmatrix} \leftrightarrow Z \begin{bmatrix} Ca^{2+} \\ Mg^{2+} \\ NH_4{}^{+} \\ K^{+} \end{bmatrix} + 2Na \tag{4}$$

One type of zeolite is clinoptilolite. Natural clinoptilolite is an inexpensive and effective cation exchanger that has a high affinity for ammonium (Koon & Kaufman, 1971). Rodriguez-Gonzalez (2017) carried out adsorption studies to determine the best ion exchanger for NH_4^{+}

removal by comparing IX capacities of clinoptilolite, vermiculite, expanded clay, glass, lava rock, plastic and sand. The results showed that clinoptilolite removed the greatest amount of NH_4^+, with a 94% removal in the absence of competing ions and 87.8% in the presence of competing ions. Results from this study also showed that the main ion exchanged with NH_4^+ on the clinoptilolite was Na^+ as clinoptilolite is naturally rich in Na^+.

One disadvantage of IX is the need for regeneration after the ion exchanger has reached its capacity. Zeolites can be chemically regenerated, usually using a brine (NaCl) solution to promote desorption of the exchanged ions back into solution as they are exchanged with Na^+. This process incurs a high cost, both for the brine itself and the treatment and disposal of the final effluent produced, which is a highly concentrated ammonium-sodium chloride solution.

Bioregeneration of the ion exchanger is an option that can decrease or eliminate the need for chemical regeneration. In this process, nitrifying biofilms utilize the NH_4^+ in the bulk liquid as an electron donor, subsequently decreasing the liquid phase NH_4^+ concentration and promoting desorption from the ion exchanger surface. Lahav and Green (1997) developed a system in which the zeolite was a carrier for nitrifying biomass. In this system, a column filled with zeolite was switched from an IX column to a fluidized bed reactor for biological regeneration upon NH_4^+ breakthrough. A sodium-enriched regenerate was still used in this system; however, the nitrified effluent produced during bioregeneration could be used in agriculture or sent for further treatment by denitrification. Bing et al. (2006) introduced clinoptilolite to an activated sludge wastewater treatment system to address the varying ammonium concentrations present within the system (30-120 mg L^{-1} as N) and the poor performance effects this produced. The addition of 50 mg L^{-1} of clinoptilolite resulted in an ammonium removal rate that was 20% better than that without clinoptilolite addition and an sCOD removal rate that was 8% better. The clinoptilolite also

improved the biodiversity of the system, as the clinoptilolite is a good biofilm carrier and maintains ammonium in the system during periods of low ammonium concentrations for the nitrifying bacteria. The system with 50 mg L^{-1} of clinoptilolite also showed much better ammonium removal under ammonium shock conditions (145 mg L^{-1} as N). The findings from these studies indicate that zeolites, such as clinoptilolite, improve the ammonia removal and nitrification performance of the nitrification stage.

To address deleterious effects of transient loadings and idle periods on substrate availability for microbial communities within PNRS, Rodriguez-Gonzalez (2017) studied the effects of adding an ion exchanger to the nitrification stage 1. Column studies were used to determine the effect of hybrid IX and BNR in a nitrification trickling filter by comparing a column with an ion exchanger (HABiTS) to a column without an ion exchanger (BNR). Clinoptilolite was used in the HABiTS column and it achieved an NH_4^+ removal of over 80% compared to 73% in the BNR column (effluents from both columns were fed to separate SOD columns for denitrification). The HABiTS column was also shown to have a quicker startup time due to the adsorption of the NH_4^+ to the clinoptilolite, and was shown to perform better after idle periods.

Additional adsorptive surfaces used in water/wastewater include, but are not limited to, Granular Activated Carbon (GAC) for the removal of organics in drinking water (Crittenden et al., 2012), biosorbents, such as biochar, for the removal of heavy metals (Inyang et al., 2012), and scrap tire for NO_3^- adsorption (Lisi et al., 2004; Krayzelova et al., 2014). Lisi et al. (2004) used granulated tire as an adsorbent for NO_3^- for the treatment of runoff from putting greens. Batch adsorption studies and the Langmuir adsorption model were used to determine a maximum nitrate loading capacity (Q_{max}) of 0.338 mg NO_3^-- N per g^{-1} of crumb tire. The study found an overall NO_3^- reduction of 58.6% in the field plots with crumb rubber compared to those without. Krayzelova et

al. (2014) developed a novel Tire-Sulfur Hybrid Adsorption Denitrification (T-SHAD) process using scrap tire for NO_3^- adsorption and some organic carbon addition, oyster shell for alkalinity, and elemental sulfur (S^0) for SOD. This process was designed to address transient nitrate loading conditions characteristic of OWTS. Adsorption studies were used to determine a higher Q_{max} of 0.657 mg NO_3^-- N per g^{-1} of scrap tire with a better fit to the Freundlich equation (sum of square value of 0.001 compared to 0.004 for Langmuir). This result was used to design column studies, which achieved NO_3^- removal efficiencies of up to 94% and was used to estimate the adsorption capacity for the scrap tire in this study (Krayzelova et al., 2014).

2.2.3 Recirculation

Recirculation can enhance treatment in PNRS in several ways: i) by promoting pre-denitrification by combining stage 1 nitrification effluent with high-cBOD septic tank effluent (STE), ii) increasing mass transfer of ammonia and oxygen to the biofilm by increasing flow velocity through the stage 1 nitrification filter due to a higher flow rate through the filter, iii) decreasing the cBOD to Total Kjeldahl Nitrogen (TKN) ratio in the stage 1 nitrification filter influent, which promotes establishment of nitrifying bacteria in stage 1 nitrification by reducing their competition with heterotrophs (Rittman & McCarthy, 2001).

Hazen and Sawyer (2015) investigated seven different full-scale prototype PNRS and found that the system with 3:1 nitrification stage 1 effluent recirculation resulted in the greatest mean TN removal (61%) and concluded that this was due to pre-denitrification from the combination of the nitrified effluent with the high-cBOD septic tank effluent (STE). The next highest TN removal observed in the study was in an in-ground stacked biofilter with single-pass nitrification stage 1 (48%).

2.2.4 Passive Nitrogen Reduction Systems

In response to the water quality degradation in the Florida Keys which was caused, in part, by nutrient loading from aging septic systems, Anderson et al. (1998) conducted a study of five different alternative systems to see if the alternative OWTS were capable of meeting advanced wastewater treatment (AWT) standards of 5 mg L^{-1} of cBOD and Total Suspended Solids (TSS), 3 mg L^{-1} of Total Nitrogen (TN), and 1 mg L^{-1} of Total Phosphorus (TP). Each system received influent wastewater from the same source and was fed at 200 gallons/day with peaks in the morning and early evening. The following treatment configurations were tested:

1) A recirculating sand filter system with an anoxic nitrification stage 2 and an unlined drip irrigation bed.
2) Septic tank effluent drains to a natural drip irrigation field sitting atop a lined bed comprised of crushed red brick, silica sand, and expanded clay, which promotes nitrification and plant uptake on top and denitrification and adsorption of phosphorus on the bottom (the most passive of the systems).
3) A fixed-film activated sludge aerobic system, which required aeration and does not address phosphorus.
4) A continuous feed cyclic reactor using a suspended growth biological treatment process in which cyclical aeration is carried out, promoting fluctuating aerobic and anaerobic conditions.
5) A rotating biological contactor disc followed by an anoxic bio-filter.

Table 2.1 shows average TN results from the five systems listed above during the study. None of the systems achieved an effluent average TN of under 10 mg L^{-1} as N.

Table 2.1. Average TN results from Anderson et. al. (1998) in mg L^{-1} as N

Influent	1	2	3	4	5
38.45 ± 10.67	20.76 ± 5.61	21.15 ± 11.27	10.97 ± 4.05	15.46 ± 6.60	12.52 ± 5.98

Although none of the systems met the AWT standards for TN, the fixed-film activated sludge system (3) had the best average removal efficiency for TN, at 71%. The drip irrigation field with the subsurface liner containing brick (2) removed the most TP and met the AWT standards, with 0.6±0.23 mg L^{-1} TP in the effluent and an average removal efficiency of 92%. This study set the standard for AWT studies in OWTS and showed that TN removal efficiencies greater than 70% are achievable without an addition of carbon in these systems.

Recently, two-stage (nitrification then denitrification) Passive Nitrogen Reduction Systems (PNRS) have been tested for their nutrient removal efficiency. Hazen and Sawyer (2014 & 2015) determined that two-stage biofiltration systems show both effective nitrogen removal and ease of implementation in single-family residences via pilot and full-scale prototype systems operated over a two year period. These two-stage systems treated the septic tank effluent first with an aerobic stage for nitrification and then with an anoxic stage for denitrification. Hazen and Sawyer, 2014 conducted pilot-scale studies using expanded clay, clinoptilolite and sand as the media for stage 1 to evaluate the effect of ion exchange and determine the best option for full-scale implementation. Pilot stage 1 biofilters were constantly fed from a septic tank via drip irrigation at a loading rate of 0.80 gal d^{-1} ft^{-1}. Idle times or transient loadings were not evaluated in this pilot study. No significant difference in treatment efficiency was observed between clinoptilolite and expanded clay biofilters, so expanded clay was chosen for implementation in stage 1 in the full-scale prototype systems due to cost.

Clinoptilolite is an ion exchange media which adsorbs ammonium ion and aids in removal during nitrification stage 1. This process also helps maintain the system during low loading periods, in which the ions are desorbed to the liquid and are used to maintain the microbial population and remove greater amounts of nitrogen (Rodriguez-Gonzalez, 2017). Sprynskyy et al. (2005) found that a naturally occurring zeolite mordenite, which is like clinoptilolite except for its crystalline structure, showed efficient removal of ammonium. The performance was improved during periods of lower loading rates and interruptions in flow. It is important to take idle times into account when designing a system for residential use. The clinoptilolite media allows nitrification systems to perform well under transient loading and after idle times, as the clinoptilolite provides a good biofilm carrier and maintains adsorbed ammonium within the system to keep the nitrifying microbial population alive during idle times. Rodriguez-Gonzalez (2017) determined the adsorption capacity of clinoptilolite to be 14 mg NH_4^+/g of material and clinoptilolite dosing was determined based on the amount needed to withstand 14 days of treatment without occurrence of BNR in that same study, which would allow for recovery of microbial populations after long idle times.

The media for denitrification stage 2 pilot studies used by Hazen and Sawyer (2014) included elemental sulfur, used as the electron donor for autotrophic denitrification or lignocellulosic material (Southern yellow pine) as the carbon source for heterotrophic denitrification and oyster shell as an alkalinity source. The pilot systems utilizing the sulfur media in stage 2 showed a better, more consistent performance (74-100% NO_x-N removal efficiencies) than those using the lignocellulosic material (41-100% NO_x-N removal efficiencies). SOD using sulfur and oyster pellets alone produces high amounts of sulfate

2.2.5 Oyster Shell as an Alkalinity Source

Sengupta et al. (2007) demonstrated that oyster shells were a better pH buffer for autotrophic denitrification in an SOD system compared with limestone and marble chips. The oyster shell in the study was found to exhibit a higher rate of alkalinity release during acid titration tests. Using XRD analysis, it was determined that oyster shell contained more calcium carbonate ($CaCO_3$), or alkalinity, in the crystalline phase than limestone, which gives oyster shell a twofold advantage of both a greater conservation of $CaCO_3$ and minimized dissolution of the material, leading to lower effluent turbidity and a longer lifetime within the system than limestone. This reduces the buildup of precipitate and turbidity within the system, and, in turn, the frequency of maintenance needed. Moon et al. (2006) studied the effects of initial alkalinity and alkalinity source (calcite, dolomite and oyster shell) on the performance of an SOD system. Results showed initial dissolution rates were lowest for oyster shell (14 mg $CaCO_3$ L^{-1} d^{-1}) and the use of oyster shell promoted the most NO_3^- removal of the three sources (98.4, 95 and 85% NO_3^- removal for oyster shell, calcite and dolomite, respectively).

2.2.6 Hybrid Adsorption and Biological Treatment Systems

To address the transient loading rates to OWTS during the denitrification stage 2 and to decrease the effluent sulfate levels, Krayzelova et al. (2014) developed and tested a novel Tire-Sulfur Hybrid Adsorption Denitrification process (T-SHAD). The media used in T-SHAD is scrap tire chips, elemental sulfur pellets, and oyster shells. This system combines BNR and nitrate (NO_3^-) adsorption to scrap tire chips to maintain the microbial community during idle times. The tire chips also provide an organic carbon source for mixotrophic denitrification. During adsorption studies, the tire chips were shown to have a nitrate adsorption capacity of 0.66 g NO_3^--N/kg of scrap tires. In flow-through column studies comparing a T-SHAD column to a tire chip only

column, Krayzelova et al. (2014) found that 18% of denitrification efficiency in the system is due to heterotrophic denitrification using organic carbon released from tire chips. The system was found to achieve a 90% removal efficiency for nitrate under steady state conditions, an 89% removal efficiency under variable flow conditions, and a 94% removal efficiency under variable concentration conditions. The highest effluent sulfate concentration of the T-SHAD system during a 30-day microcosm study was around 140 mg L^{-1} compared to 350 mg L^{-1} in the effluent from the sulfur and oyster shell only microcosm during the same study.

Some concerns have been raised regarding potential environmental impacts of using scrap tire chips in OWTS. However, a report by Shulluck (1990) was carried out to analyze the environmental impacts of using shredded scrap tires instead of crushed stone in onsite systems determined that leachate from the scrap tire material would not contribute a significant amount of pollution to the groundwater. Nelson et al. (1994) found that, out of 118 toxic organic chemicals tested in tire chip leachate, none reached concentrations exceeding 1 ng L^{-1}. Kellough (1991) tested tire leachate for 28 metal elements, 28 PCB compounds, and 18 PAH compounds and found that scrap tires release low amounts of all compounds tested. Therefore, scrap tire material is viable for use in advanced OWTS.

HABiTS is a novel advanced OWTS which utilizes clinoptilolite and expanded clay in the nitrification stage 1 and the T-SHAD system for the denitrification stage 2 (Rodriguez-Gonzalez et al., 2017). It has been shown to be effective for the removal of nitrogen in bench scale experiments, especially at higher and transient loading rates. The two-stage system, which incorporates IX with the clinoptilolite and adsorption on the tire chips of ammonia and nitrate, respectively was proposed to address the variable loading rates and long idle times which are characteristic of onsite systems and can influence the BNR processes within them.

Stage 1 effluent recirculation can also enhance treatment within the system by pre-denitrification occurring in the recirculation tank. Hazen and Sawyer (2015) observed significant pre-denitrification in their BHS-2 system, which had stage 1 effluent recirculation in a 2-stage system with Stage 1 nitrification (expanded clay) then Stage 2 denitrification (lignocellulosic followed by SOD), as this system had the highest Total Nitrogen (TN) removal in stage 1 (61%).

2.3 Materials and Methods

2.3.1 System Configuration and Influent Feeding

Two side-by-side systems with the same media compositions (R and FF) were fed screened raw wastewater from the Northwest Regional Water Reclamation Facility in Tampa, Florida via a single, septic tank. The recirculation system used two submersible pumps (located in the recirculation tank and the pump tank), while the forward flow system used one. Flows were regulated by a timer and tank levels were maintained by float valves in the influent to the septic tank and the pump tank. A schematic of the systems is shown in Figure 2.1 and details on all system components can be found in Table 2.3.

2.3.2 Media Materials

Expanded clay (Trinity Lightweight, Livingston, AL), clinoptilolite (St. Cloud Mining Company, Winston, NM) and oyster shell (Shell's Agricultural Supply, Tampa, FL) were used in stage 1 nitrification and tire mulch (Liberty Tire Recycling, Rockledge, FL), elemental sulfur (Southern Aggregates, Palmetto, FL) and oyster shell (Myco Supply, Pittsburgh, PA) were used in stage 2 denitrification. The characteristics and composition of media materials used in the two stages are listed in Table 2.2.

2.3.3 System Components

The pilot scale system is shown schematically in Fig. 2.1. A complete list of all system components, quantities, manufacturers, and dimensions (when applicable) is shown in Table 2.3.

2.3.4 Startup

The septic tank was filled with screened raw sewage from Northwest Regional Water Reclamation Facility on July 26, 2017. Nitrification stage 1 startup occurred on August 1, 2017. For startup of nitrification stage 1, 2.5 gallons of Mixed Liquor Suspended Solids (MLSS) from the oxidation ditch at the plant were applied to the top of each stage 1 biofilter and they were filled with screened raw sewage for 4 hours in order to speed up the acclimation period of nitrifiers in the filter. The MLSS was also acquired from Northwest Regional Water Reclamation Facility, which uses a 5-stage Bardenpho process with an integrated carousel.

Startup of denitrification stage 2 occurred on August 14, 2017 (day 14). MLSS was not added to this stage, as biomass carryover from nitrification stage 1 was assumed to be significant enough for inoculation of denitrification stage 2.

2.3.5 Operation

Due to a hydraulic issue during the first 49 days of operation, forward flow rates were, on average, 15.3 gallons d^{-1} for FF-system and 26.4 gallons d^{-1} for R-system and forward flow loading rates of 2 gallons d^{-1} ft^{-2} and 3.72 gal d^{-1} ft^{-2} to stage 1 filters, respectively, as the Recirculation Tank had to be filled daily to keep up with the recirculation pump capacity. During this time, R-system operated at a 7:1 recirculation rate. On day 50, new timers were installed and flow was restored to 35.5 gal d^{-1} per system as described below. The flow rate change is indicated by a vertical line at day 50 in all daily variation results. This flow rate would be equivalent to 88.75 gal d^{-1} in a full-scale system with a 1000 gallon septic tank.

This resulted in Septic tank effluent (STE) being applied at a forward flow loading rate of 5 gallons ft^{-2} d^{-1} to stage 1 biofilters. Flow was divided under the National Sanitation Foundation Standard 40 for variable loading where 35%, 25% and 40% of the daily volume was distributed between 6 to 9am (6 doses), 11 to 2pm (8 doses) and 6 to 9pm (6 doses), respectively, totaling 20 doses throughout the day (NSF 2013). Hydraulic retention times (HRTs) for FF-system and R-system at the two flow rates are listed in Table 2.4. Day 1-49 represents the time when the flow rate was low and day 50-59 is the period in which it was corrected.

2.3.6 Sample Analysis

Chemical analysis was done on equipment in the USF Environmental Engineering laboratory. Anions (Cl^-, NO_3^-, NO_2^-, PO_4^{3-}, SO_4^{2-}) (D4327-11) and cations (Na^+, NH_4^+, Mg^{2+}, Ca^{2+}, K^+) (D6919-17) for all experiments were measured by Ion Chromatography with chemical suppression of eluent conductivity (Dionex, 2001) with a Metrohm 850, Professional Ion Chromatograph (Dionex, 2001) according to the Standard Methods (D4327-11 and D6919-17, respectively, APHA et al., 2012). Method Detection Limits (MDLs) (in mg L^{-1}) for NO_3^-, NO_2^-, PO_4^{3-}, and SO_4^{2-} were 0.01, 0.04, 0.02, and 0.01, respectively. An Oakton (Vernon Hills, IL) pH 2700 benchtop meter with an Orion 5 Star Meter Probe (calibrated) was used for measurements of pH, Conductivity, and Alkalinity (weekly) according to the Standard Methods (4500 H+B, 2510 B, 2320 B, respectively, APHA et al., 2012). An Oakton (Vernon Hills, IL) DO 110 meter with a calibrated electrode was used for dissolved oxygen measurements in the field according to the Standard Methods (4500-O G, APHA et al., 2012).

Chemical Oxygen Demand (COD) on filtered and unfiltered samples was measured weekly using Lovibond COD vials (Amesbury, England) (MDL 0-150 mg L^{-1}) according to the Standard Methods (5220 C; APHA et al., 2012). HACH TNTplus 827 kits were used to measure total

nitrogen (5-40 mg L^{-1} as N) and HACH TNTplus 844 kits were used to measure total phosphorus (MDL 1.5-15 mg L^{-1} as P) (HACH, Loveland, Colorado). Total Suspended Solids (TSS) and Volatile Suspended Solids (VSS) were also measured weekly using the Standard Methods (2540-D and 2540-E, respectively, APHA et al., 2012).

Sampling was performed five times each week from day 2 until day 31 of the study, when it was decreased to three times each week for the remainder of the study. One idle period of four days occurred during Hurricane Irma (September 8, 2017-September 12, 2017), when the system was shut off on day 39 and was re-started on day 43. After startup, performance was evaluated using methods outlined above.

2.3.7 Statistical Analysis

A two-sample T-Test assuming equal variance with a 95% confidence level was run using Microsoft Excel 2011.

Table 2.2. Media characteristics and composition of each system for nitrification stage 1 and denitrification stage 2.

Stage	**Material**	**Particle size (in)**	**Weight (lbs)**	**Percent by weight**
1	Expanded clay	0.20-0.30	244.90	82%
	Clinoptilolite	0.11-0.22	48.98	16%
	Oyster	0.25	5.51	2%
2	Tire	Variable	76.45	83%
	Sulfur	0.25	12.23	13%
	Oyster	0.25	3.98	4%

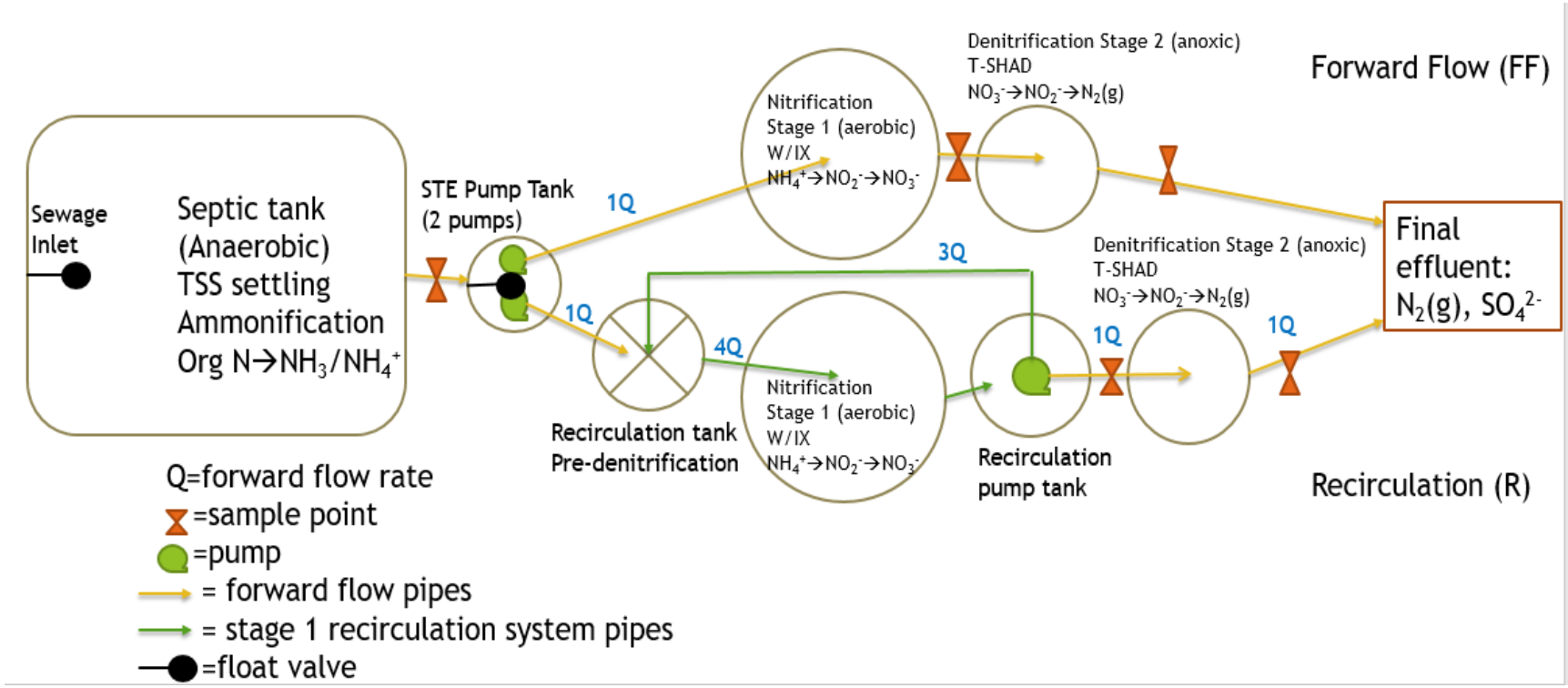

Figure 2.1. Schematic of the two side by side systems (R and FF) and septic tank. Flow directions are indicated by arrows. Not drawn to scale.

Table 2.3. Pilot system component descriptions and manufacturers

Component	**Quantity**	**Manufacturer**	**Item**	**Spray painted?**	**Tank Volume**	**Dimensions**
Septic Tank	1	Norwesco, Georgia, US	525 Gallon Black Heavy Duty Horizontal Leg Tank	No	525 gallons	L=5’ W=4’ H=4’
STE Pump Tank and cover	1	Tamco Industries, Lima, Ohio, US	Short Polyethylene Tank	Yes	27 gallons	D=22” H=18”
Recirculation Tank	1	Rubbermaid, Fairlawn, Ohio, US	Roughneck trash can	No	32 gallons	D=20” H=25”

Table 2.3 (Continued)

Stage 1 tanks	2	Ace Roto-Mold, Iowa, US	White Open Top Containment Tank	Yes	145 gallons	D=36” H=39”
Recirculation Pump Tank	1	Rubbermaid, Fairlawn, Ohio, US	Roughneck trash can	No	40 gallons	D=22” H=30”
Stage 2 tanks	2	TR Drum, LLC, Plant City, Florida, US	Dot Open Top Plastic Tank	No	55 gallons	D=23” H=36”
Forward Flow Pumps	2	EcoPLUS, Vancouver, BC, Canada	6.6 GPM Fixed Flow Submersible/Inline Pump	N/A	N/A	Connection diameter=1/2”
Recirculation Pump	1	Superior Pump, Minneapolis, Minnesota, US	26 GPM (1-1/4”) Submersible Utility Pump	N/A	N/A	Connection diameter=3/4”
Recirculation Valves	2	Asahi, US	Omni Type 27 Ball Valve PVC	N/A	N/A	3/4" Threaded
In-line Sampling Valves	4	King Brothers, Valencia, CA, US	Ball Valve PVC	N/A	N/A	3/4" Threaded
Sampling Valves	6	King Brothers, Valencia, CA, US	Ball Valve PVC	N/A	N/A	1/2" Threaded
Pipe	N/A	Charlotte Pipe, Charlotte, NC, US	PVC Schedule 40	No	N/A	D=1”
Tubing from STE pumps to Stage 1/Recirculation Tank and Final Effluent	40’	Ace Hardware, Oak Brook, IL, US	Clear Acrylic Tubing	Yes	N/A	D=3/4”
Float Valves for Septic Tank Influent and Pump Tank (STE)	2	Grainger, Tampa, Florida, US	Float Ball Round Plastic Float Valve In-Line PVC Float Rod	N/A	D=5” D=3/4” L=6”	
Timers for Forward Flow and Recirculation pumps	2	ChronTrol, San Diego, California, US	XT-4	N/A	N/A	

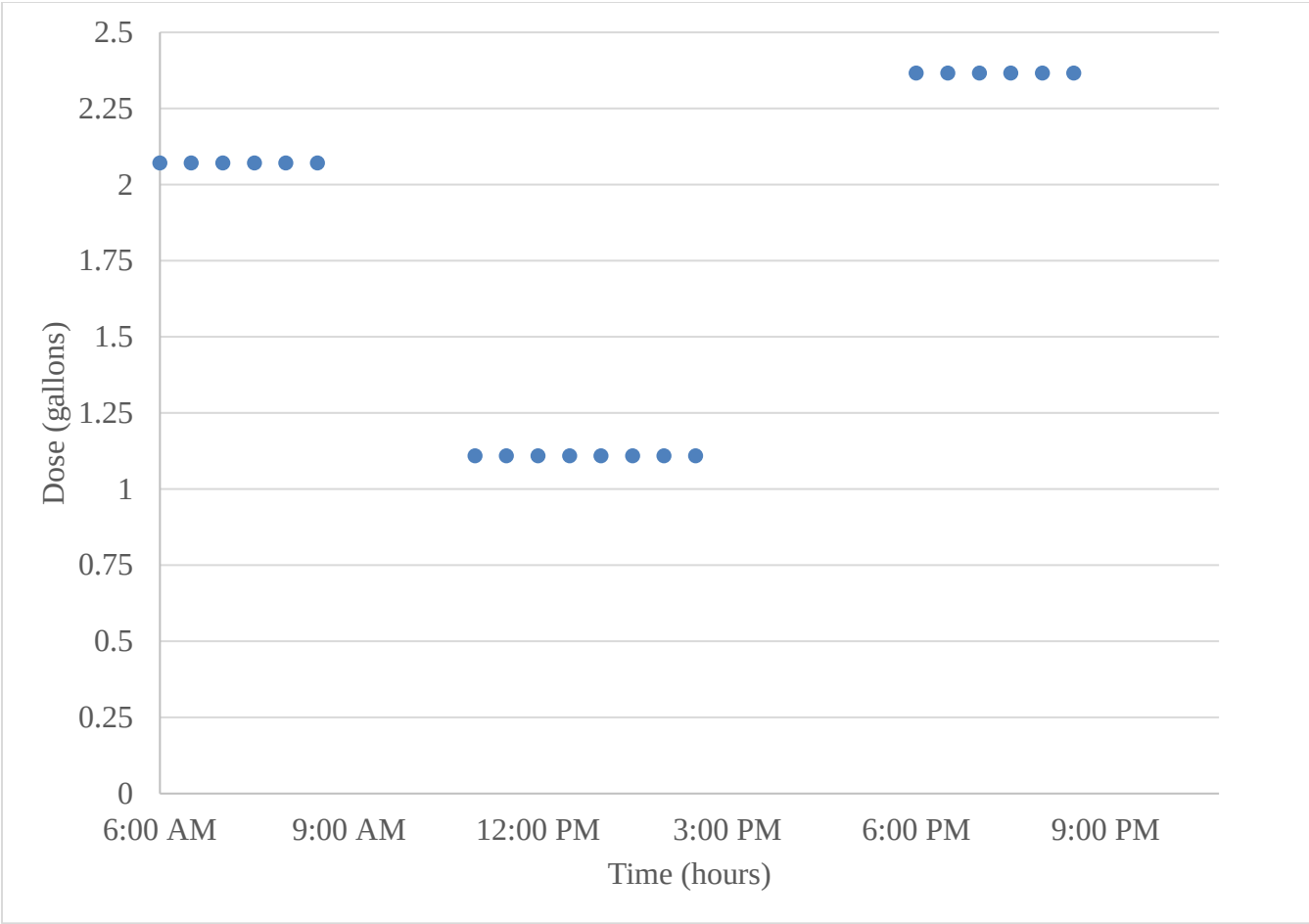

Figure 2.2. Dosing schedule for pilot system (FF-system and R-system) at the 35.5 gallon d^{-1} flow rate.

Table 2.4. HRTs of each stage throughout the study calculated by Empty Bed Contact Time (EBCT)

Day	Septic tank	R-1	FF-1	R-2	FF-2
1-49	9.6 d	4.9 d	5.2 d	1.9 d	3.2 d
50-59	5.7 d	3.65 d	2.2 d	1.4 d	1.4 d
Bench scale HABiTS under moderate loading (5.15 gal ft^{-2} d^{-1})			2.91 d		0.58 d

2.4 Results and Discussion

2.4.1 Nitrification Stage 1 Performance

Figure 2.2 shows NH_4^+-N, Na^+, NO_2^- -N, NO_3^- -N and TIN in mg L^{-1} from the influent to stage 1 (STE) and effluent to nitrification stage 1 for the recirculation (R-1) and forward flow (FF-1) systems for the first 58 days of the study (8/2/2017-9/27/2017). R-1 had a higher NH_4^+ removal efficiency (87%) compared to FF-1 (70%). Effluents from R-1 consistently showed lower NH_4^+ and higher NO_3^- concentrations (Fig. 2.2 a and d), which could be attributed to enhanced nitrification activity from lower BOD:TKN ratio in the influent and/or higher mass transfer from increased turbulence caused by the higher flow rate in nitrification stage 1 due to recirculation.

Figure 2.2 b shows sodium (Na^+) concentrations throughout the study. Rodriguez-Gonzalez (2017) showed that Na^+ is the main ion exchanged with NH_4^+, so the initial spike in Na^+ concentration was expected as the clinoptilolite adsorbs NH_4^+ from the influent and desorbs Na^+, indicating that most of the initial NH_4^+ removal is due to IX. Clinoptilolite used in this study was not pre-treated so initial Na^+ concentrations were around 50 mg L^{-1} higher than those observed in the column study by Rodriguez-Gonzalez (2017), which used a similar media composition in nitrification stage 1. After the initial Na^+ spike, a NO_2^- spike around day 10 shown in Figure 2.2 c

indicates the presence of nitrification, as NO_2^- is an intermediate in biological nitrification. The lag in the initial biological activity may be explained by high Na^+ concentrations, as Na^+ is inhibitory to nitrification at high concentrations (Sanchez et al., 2004). NO_2^- -N concentrations were around 5 mg L^{-1} higher at the peak for R-1 compared to FF-1. This could have been due to higher mass transfer in the R-1 filter or enhanced nitrifying biomass growth, mentioned in conjunction to nitrification above. After the initial acclimation phase, most of the influent NH_4^+ was converted to NO_2^- and NO_3^- in both R-1 and FF-1.

A significant drop in NO_3^- was observed around day 50 for R-1 (Fig. 2.2 d). This could be explained by the increase in forward flow rate, which brought the recirculation ratio from 7:1 to 3:1. This adjustment increased the retention time in the recirculation tank, causing anoxic conditions in the tank, which would promote pre-denitrification. Pre-denitrification in the recirculation tank can explain the divergence in TIN concentrations between R-1 and FF-1 filter effluents shown in Figure 2.3 e. Table 2.5 shows average nitrogen species from influent and stage 1 of each system for the duration of the study. Differences in average NH_4^+-N are statistically significant (α=0.05) and indicate enhanced nitrification in the R-1 filter compared to FF-1. Table 2.7 shows overall TIN removal efficiencies for the two stages in R-1 and FF-1. Most of the TIN removals in FF-1 and R-1 can be attributed to IX on the clinoptilolite, as this process retains the NH_4^+ in the system. The difference between TIN removal efficiencies in R-1 and FF-1 can be attributed to some pre-denitrification in the recirculation tank before nitrification stage 1, as the influent to this tank is nitrified effluent from the R-1 nitrification stage 1 filter and STE, which has a substantial amount of sCOD. Pre-denitrification could also be indicated by lower sCOD concentrations in nitrification stage 1 effluent, however the differences between R-1 and FF-1 average sCOD were not significant. The occurrence of pre-denitrification in the R-1 filter was

confirmed by an ion balance on ions exchanged with NH_4^+ on clinoptilolite. A simple equation was used with all units in meq L^{-1} to estimate ion desorption from the clinoptilolite:

$$(Ca^{2+} + K^+ + Na^+ + Mg^{2+})_{desorbed} = (Ca^{2+} + K^+ + Na^+ + Mg^{2+})_{out} - (Ca^{2+} + K^+ + Na^+ + Mg^{2+})_{in} \quad (5)$$

Adsorption of NH_4^+ (in meq L^{-1}) was assumed to be equal to ions desorbed from the equation above. The sum of ions desorbed was subtracted from the sum of NH_4^+ removed but not converted to NO_x (NO_2^-+NO_3^-) in meq L^{-1} and the resultant of this was assumed to be the total nitrogen removed by pre-denitrification or incorporated into biomass in nitrification stage 1. The result for R-1 (20.99 meq L^{-1}) was over double that of FF-1 (9.52 meq L^{-1})

2.4.2 Denitrification Stage 2 Performance

Denitrification stage 2 utilized a novel T-SHAD system as described previously. Denitrification stage 2 was started up on day 14 of the study and samples were taken beginning on day 17. Throughout the study, this stage removed 100% of the NO_3^- load (Figure 2.4). Some sulfate reduction was observed due to the long retention time in the biofilters, indicated by the characteristic rotten egg smell of hydrogen sulfide (H_2S) and lower sulfate concentration in stage 2 compared to stage 1 effluent (Figure 2.7). The tire chips were not pre-treated prior to their addition to the stage 2 filters, so they added a significant amount of sCOD, as shown in Figures 2.5 and 2.6. This was utilized by heterotrophic denitrifying bacteria in the reactors, which, along with SOD, contributed to the high denitrification observed in Stage 2 of both sides. Increased sulfate concentrations beginning around day 51 from stage 2 (Figure 2.5 and 2.6) could be indicative of increasing SOD or a drop in sulfate reduction due to a lower HRT in stage 2 from the increase in forward flow rate on day 51. As sCOD concentrations decrease around day 50, SO_4^{2-}-

S concentrations increase. As mentioned previously, this is most likely due to higher SOD as the heterotrophic utilization of the organic carbon from the tire chips and the higher flow rate through stage 2 caused a drop in sCOD, making organic carbon less available in the system. Krayzelova et al. (2014) observed similar results in column studies, with similar denitrification efficiencies in a tire only and a T-SHAD column occuring during the start up of the study then dropping to 18% in the tire only column compared to 90% in the T-SHAD column. This was due to the high COD concentrations observed in both columns during start up (178 and 201 mg L^{-1} for tire only and T-SHAD column, respectively).

2.4.3 Overall System Performance

Table 2.6 shows average water quality results for the entire system throughout the study. The only parameters that showed significant differences between R and FF (α=0.05) were NH_4^+-N for stage 1 and 2 and NO_2^--N for stage 1. NH_4^+-N was significantly lower in R-1 and R-2 than in FF-1 and FF-2, while NO_2^--N was significantly higher in R-1, which was possibly due to the increased nitrification efficiency from recirculation. PO_4^{3-} removal was not significant from either stage 1 or 2. However, the decrease from influent to stage 1 effluent was higher than that from stage 1 to stage 2 in both sides. R-1 and FF-1 showed similar average PO_4^{3-} concentrations. Amini et al. (2017) observed significant PO_4^{3-} removal on clinoptilolite in batch studies treating high-strength swine waste centrates (55 mg L^{-1} as P), so the small observed removal could have been due to PO_4^{3-} adsorption to clinoptilolite Neutral pH was maintained throughout the study, and average alkalinity concentrations were not significantly different from stage 1 to stage 2 for either side. This could support the occurrence of some heterotrophic denitrification as SOD alone would cause the alkalinity

concentrations to decrease. Average DO concentrations from stage 2 were 0.58±0.82 mg L^{-1} and 0.45±0.77 mg L^{-1} for R-2 and FF-2, respectively, which indicates that the stage 2 filters supported anoxic conditions, while average DO concentrations from stage 1 filters were 3.26 ±0.63 and 2.86±0.69 mg L^{-1} for R-1 and FF-1, respectively, showing that the stage 1 filters maintained aerobic conditions.

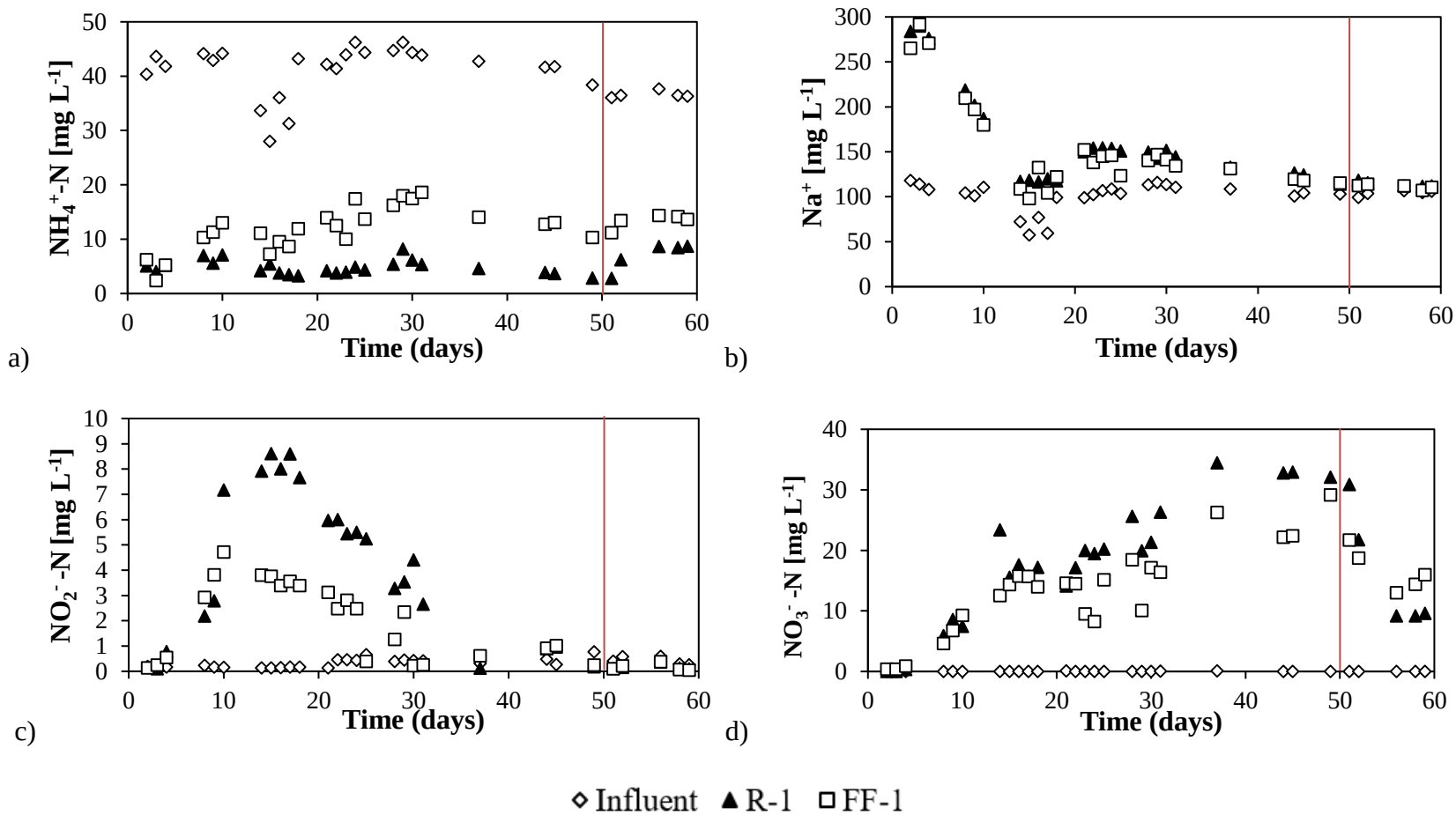

Figure 2.3. Daily variations of a) NH_4^+, b) Na^+, c) NO_2^-, d) NO_3, and e) TIN for influent, R-1 and FF-1. Line indicates day 50, when forward flow rates were increased.

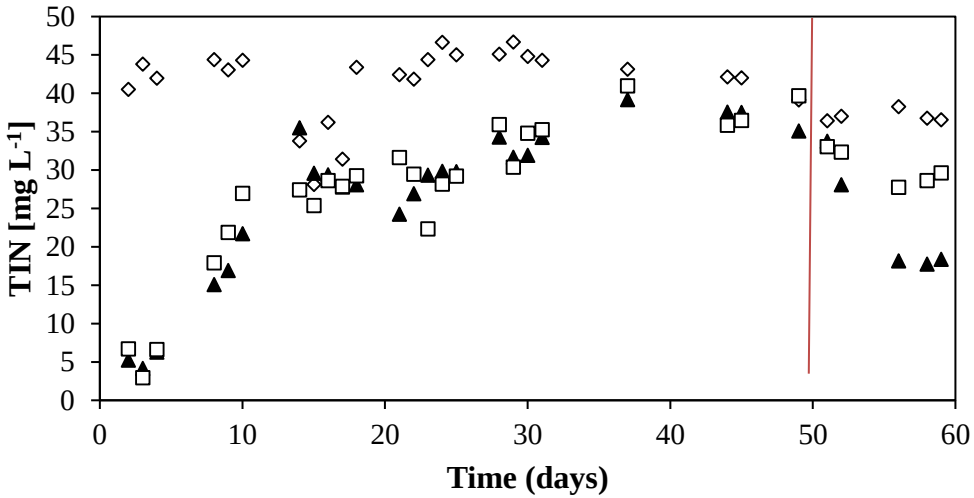

e)

Figure 2.3 (Continued)

Table 2.5. Average N species results for influent, R-1 and FF-1 biofilters for the duration of the study.

	Influent	**R-1**	**FF-1**
NH_4^+-N (mg L^{-1})	40.96 ± 4.09	5.13 ± 1.97	13.76 ± 2.72
NO_2^--N (mg L^{-1})	0.40 ± 0.16	3.06 ± 2.86	1.29 ± 1.26
NO_3^--N (mg L^{-1})	0.01 ± 0.03	21.50 ± 8.10	16.88 ± 5.37
TIN (mg L^{-1} N)	40.82 ± 4.63	25.90 ± 9.46	27.63 ± 8.92

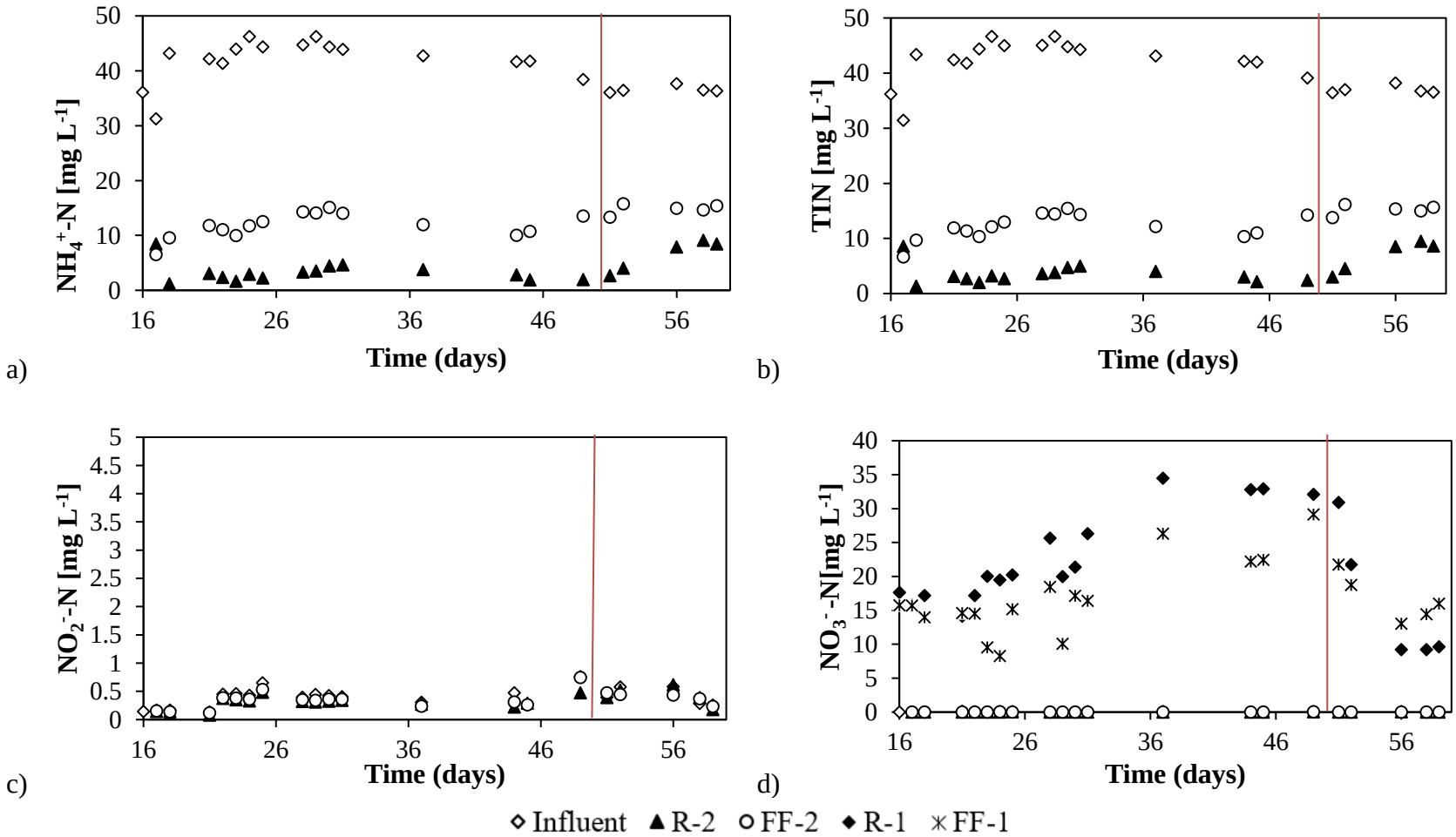

Figure 2.4. Daily variations of a) NH_4^+-N, b) TIN, c) NO_2^--N for influent, R-2 and FF-2 and d) NO_3^--N for influent, R-1, FF-1, R-2 and FF-2. Line indicates day 50, when forward flow rates were increased.

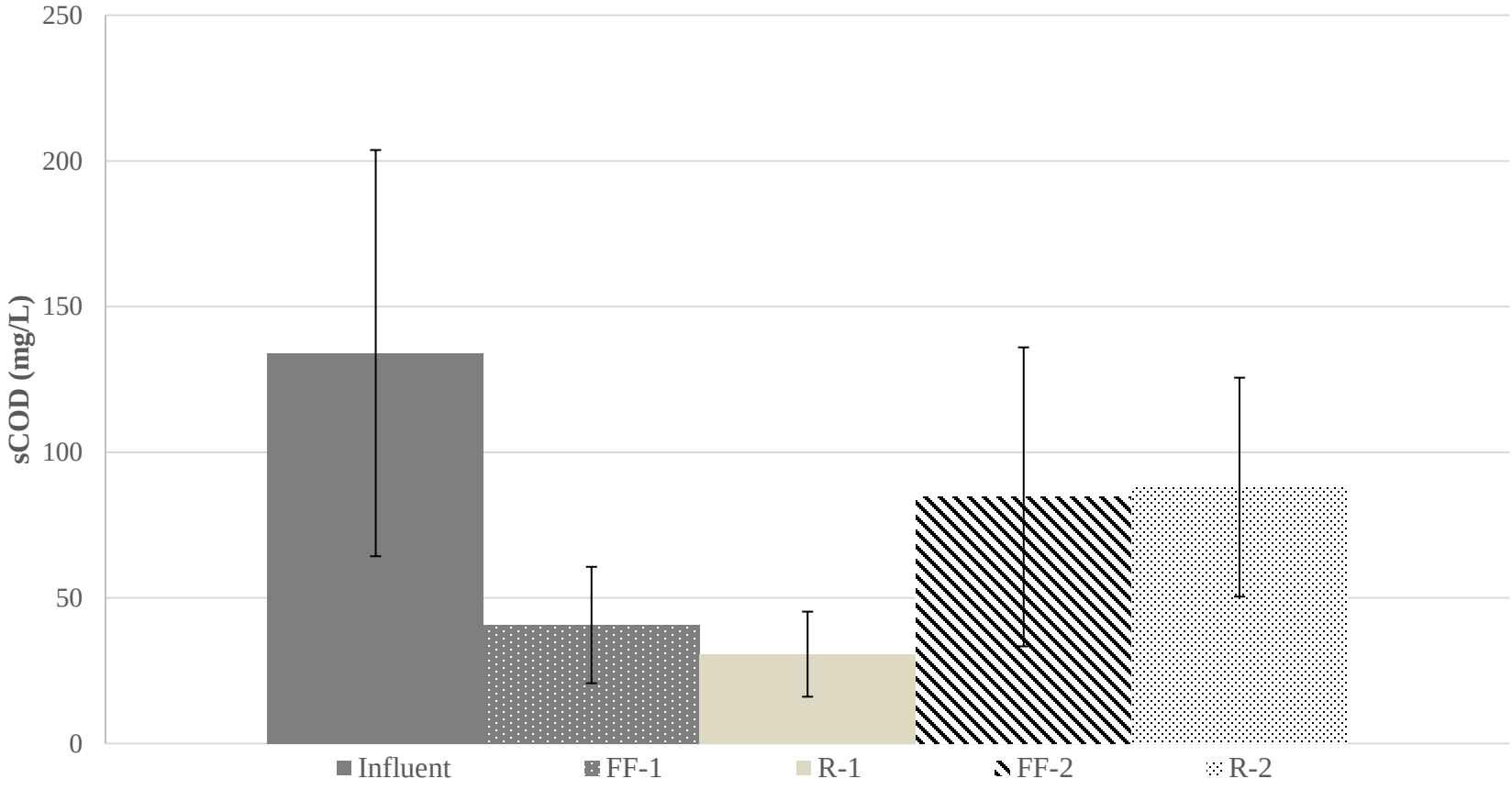

Figure 2.5. Average sCOD for influent, stage 1 and stage 2 for both systems for the duration of the study.

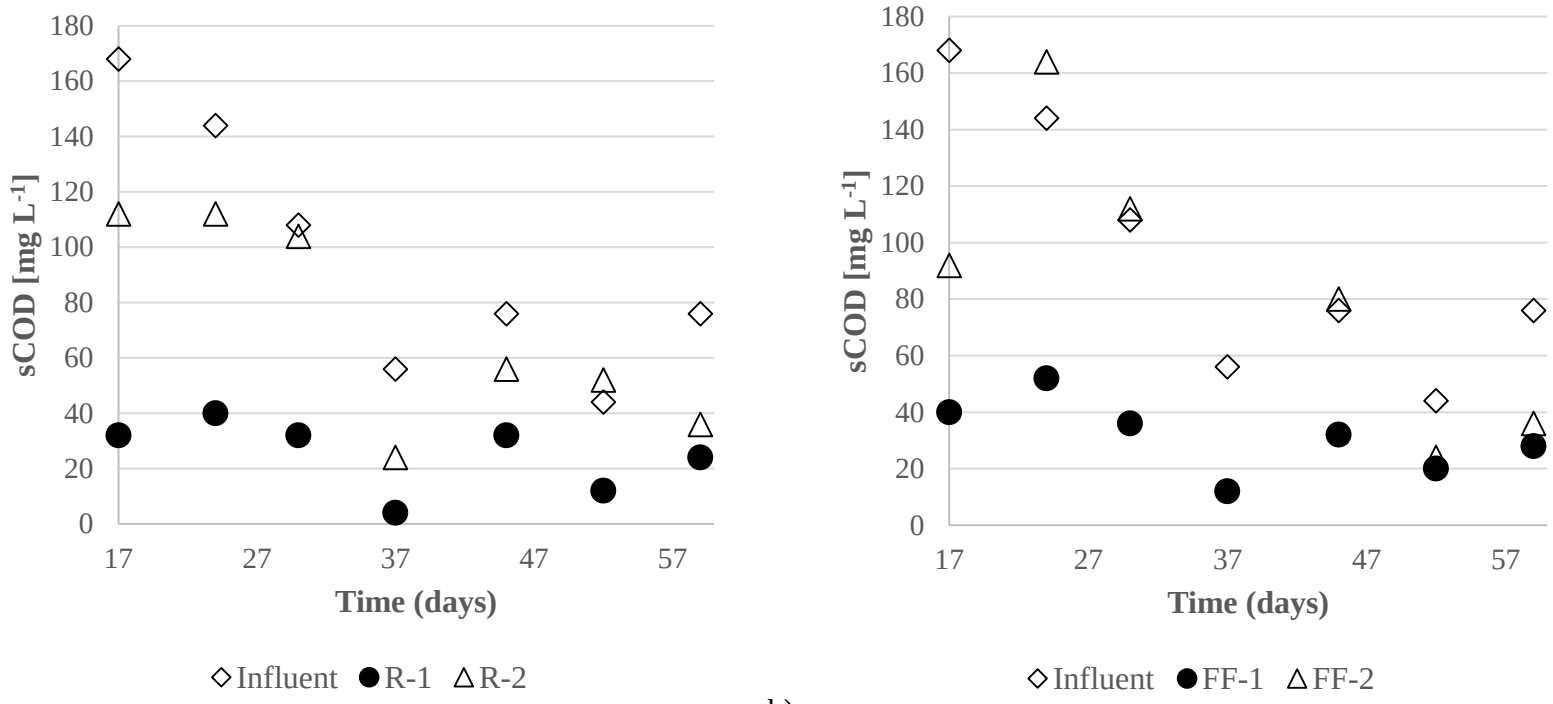

a) b)

Figure 2.6. Daily variations for sCOD for influent and effluent of stage 2 for each system: a) R-1 and R-2 and b) FF-1 and FF-2

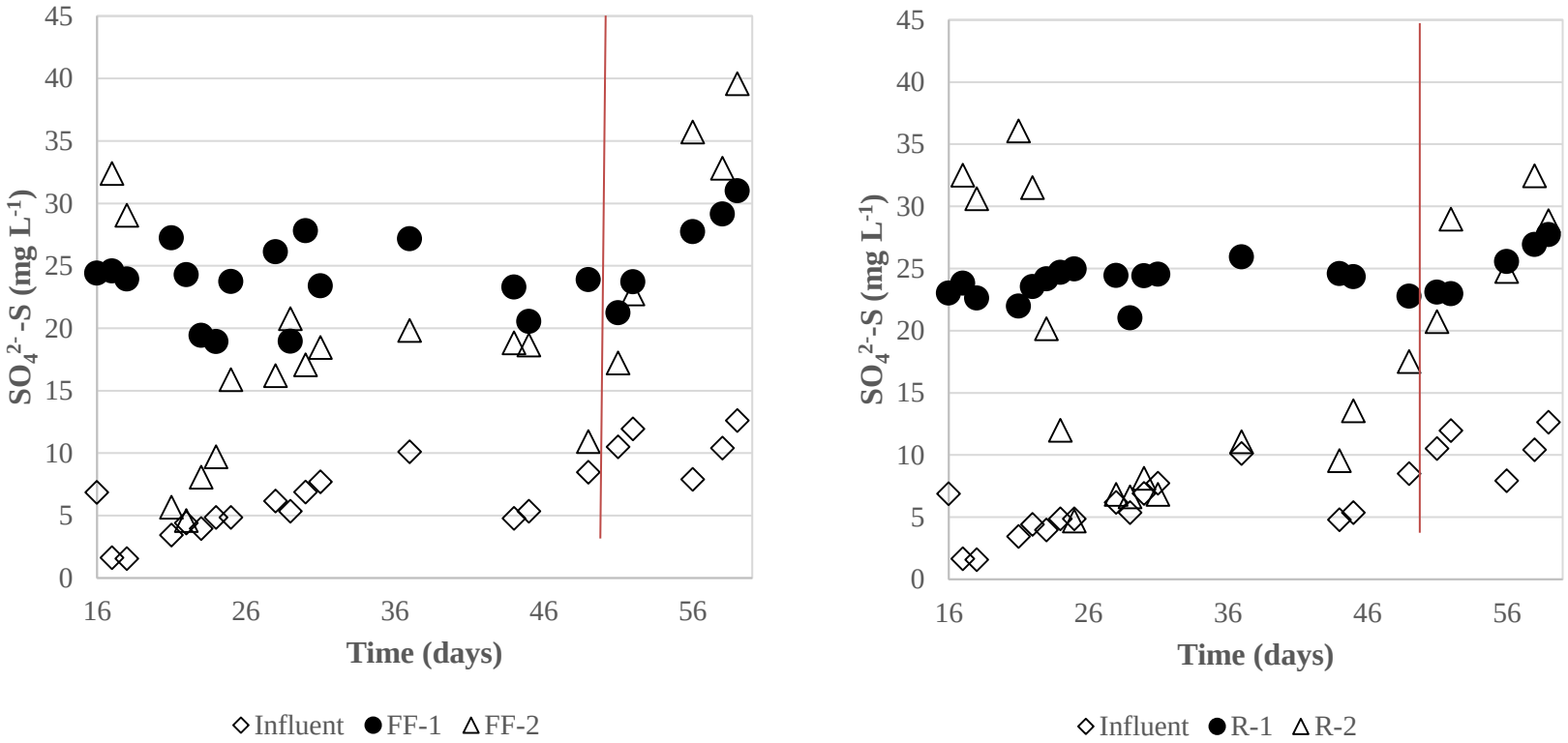

a) b)

Figure 2.7. Sulfate (as SO_4^{2-}-S) daily variations for a) influent, FF-1, and FF-2 and b) influent, R-1 and R-2 from day 16-day 58 of the study

Table 2.6. Average water quality results for influent, R-1 , R-2, FF-1 and FF-2 biofilters from day 17-day 59 of the study. R values in bold are significantly different from the corresponding FF treatment.

	Influent (STE)	**R-1**	**R-2**	**FF-1**	**FF-2**
pH	7.31 ± 0.17	7.50 ± 0.08	7.60 ± 0.34	7.65 ± 0.12	7.67 ± 0.26
DO (mg L^{-1})	0.34 ± 0.25	3.26 ± 0.63	0.58 ± 0.82	2.86 ± 0.69	0.45 ± 0.77
Alkalinity (mg L^{-1} as $CaCO_3$)	421.74 ± 50.66	274.95 ± 124.39	277.62 ± 56.86	312.08 ± 77.94	312.88 ± 88.86
NH_4^+-N (mg L^{-1})	40.96 ± 4.09	**5.13 ± 1.97**	**4.25 ± 2.47**	13.76 ± 2.72	11.67 ± 2.40
NO_2^--N (mg L^{-1})	0.40 ± 0.16	**3.06 ± 2.86**	0.33 ± 0.14	1.29 ± 1.26	0.35 ± 0.14
NO_3^--N (mg L^{-1})	0.01 ± 0.03	21.50 ± 8.10	0.00 ± 0.01	16.88 ± 5.37	0.00 ± 0.00
Na^+ (mg L^{-1})	103.43 ± 11.45	132.82 ± 17.04	134.45 ± 20.70	126.66 ± 15.20	126.13 ± 14.93
K^+ (mg L^{-1})	18.37 ± 1.66	22.45 ± 2.10	22.54 ± 2.45	25.16 ± 1.84	25.09 ± 2.11
Ca^{2+} (mg L^{-1})	168.58 ± 15.09	135.37 ± 16.61	147.48 ± 18.44	149.34 ± 15.65	152.26 ± 20.98
Mg^{2+} (mg L^{-1})	40.21 ± 4.32	39.15 ± 5.20	39.35 ± 5.57	38.80 ± 4.99	38.55 ± 4.36
Cl^- (mg L^{-1})	122.44 ± 7.22	123 ± 6.85	124.60 ± 7.65	123.96 ± 8.92	122.75 ± 6.80
PO_4^{3-}-P (mg L^{-1})	10.80 ± 2.98	9.78 ± 1.82	9.39 ± 1.96	9.70 ± 1.60	9.01 ± 1.84
SO_4^{2-}-S (mg L^{-1})	3.00 ± 1.33	23.21 ± 0.90	16.43 ± 11.36	23.89 ± 2.82	16.80 ± 7.98
sCOD (mg L^{-1})	110.40 ± 46.07	28.00 ± 14.01	88.00 ± 37.57	34.40 ± 14.31	84.67 ± 51.31

Table 2.7. Total TIN removal efficiencies from influent to effluent of R-1 and FF-1 and overall TIN removal after denitrification stage 2 (R-2 and FF-2) for the duration of the study.

Stage	**R-1**	**FF-1**	**R-2**	**FF-2**
TIN removal efficiency (%)	35.4	28.8	88.8	54.9

2.5 Conclusions

The first objective of this study was to evaluate the startup performance of a pilot scale HABiTS system. Na^+, NO_2^- and TIN results from nitrification stage 1 indicate that IX dominated the first 10 days of the study, or the startup period, and then biological processes started up, shown by the initial spike in NO_2^-. In denitrification stage 2, high initial sCOD concentrations and long HRTs on both sides promoted complete denitrification and some SO_4^{2-} reduction. As the study progressed, a rise in SO_4^{2-} concentrations indicated SOD and/or decreasing SO_4^{2-} reduction due to an increase in the forward flow rate from day 50.

The other objective was the investigation of the effect of nitrification stage 1 effluent recirculation on the performance of the system. Due to a hydraulic issue, the nitrification stage 1 effluent recirculation ratio from day 1-49 of the study was 7:1, until it was corrected to 3:1 on day 50. However, higher NH_4^+-N removal was observed in R-1 (87%) compared to FF-1 (70%) via a combination of nitrification and IX in both systems. Higher TIN removal was observed in R-1 (35.4%) compared to FF-1 (28.8%), indicating that pre-denitrification was a significant removal mechanism in the R-1 filter. Overall TIN removal efficiencies for R (88.8%) were much higher than those for FF (54.9%). This could be attributed to pre-denitrification in R-1 along with lower BOD:TKN ratios in the R-1 filter influent and higher mass transfer in the R-1 filter from recirculation, which both contributed to higher nitrification rates in R-1 compared to FF-1. The R

system also had TIN concentrations below 10 mg L^{-1} during the sampling time throughout the study, while FF final effluent had an average TIN concentration of 12.90 ± 2.47 mg L^{-1}.

CHAPTER 3: ANALYSIS OF BIOFILM DISTRIBUTIONS IN PARTICULATE PYRITE AUTOTROPHIC DENITRIFICATION PROCESS WITH AND WITHOUT OYSTER SHELLS

3.1 Introduction

As some conventional Onsite Wastewater Treatment Systems (OWTS) do not adequately remove nitrogen, additional treatment can be necessary to prevent detrimental environmental effects. Effluent from the septic tank is high in ammonium (NH_4^+), which oxidizes to nitrate (NO_3^-) in the soil treatment system (USEPA, 2002). NO_3^- is highly soluble and mobile in soil and groundwater, so it is easy for groundwater and surface water NO_3^- contamination to occur, especially areas of poor soil and/or bedrock such as the Florida Keys (Lapointe et al., 1990). Sulfur Oxidizing Denitrification (SOD) is an effective treatment method for NO_3^- that produces less sludge than heterotrophic denitrification and has been used in multiple studies on its own or in combination with other treatment methods (FOSNRS, 2015; Krayzelova et al., 2014; Rodriguez-Gonzalez et al., 2017). Disadvantages of SOD are high sulfate production and alkalinity consumption (Pu et al., 2014).

An alternative electron donor for autotrophic denitrification is pyrite. Tong et al (2017a) compared the Particulate Pyrite Autotrophic Denitrification (PPAD) system, which includes pyrite as an electron donor, oyster shell as an alkalinity source and sand as a biofilm carrier to SOD and found that PPAD denitrification rates (0.86 mg L^{-1} h^{-1}) were close to those of SOD (1.19 mg L^{-1} h^{-1}). PPAD also produced less sulfate compared to SOD (4.57 g SO_4^{2-}/g NO_3^-- N compared to 7.54 g SO_4^{2-}/g NO_3^-- N) and consumes less alkalinity (1.7 g $CaCO_3$/g NO_3^-- N compared to 4.54 g

$CaCO_3$/g NO_3^-- N). The lower alkalinity consumption of PPAD makes an additional alkalinity source unnecessary if the influent to the system has sufficient alkalinity, however oyster shells may have some other benefits to the system such as biofilm carrying capacity and growth of nitrifying bacteria (Ivanov et al., 2006).

Tong et al. (2017b) investigated the effect of oyster shells on the PPAD process by comparing two side-by-side columns, one with oyster shells (P+S+OS) and one without (P+S). Table 3.1 shows the experimental phases and overall TIN removal efficiencies for each phase. In Phase I of the experiment, the column without oyster shell performed better than the column with (NO_3^--N removal efficiencies of 58.1% and 39.8%, respectively). In Phase III, organic substrate was added with the addition of 10% by volume of settled domestic wastewater. During this phase, the Total Inorganic Nitrogen (TIN) removal efficiency of the P+S column decreased to 42.4% and increased in the P+S+OS column to 43.8%. Based on this result, it was concluded that the oyster shells supported some heterotrophic denitrifying bacteria, which allowed it to improve in performance with the addition of the organic carbon, while the P+S column did not. This was supported by an increase in alkalinity in the P+S+OS column, (325 mg L^{-1} in Phase I to 350 mg L^{-1} in Phase III) which is indicative of heterotrophic denitrification, as this process produces some alkalinity. When the flow rate was decreased from 1 L/d to 0.6 L/d in order to increase the residence time to around 6 hours in Phase IV, the TIN removal efficiency in both columns was improved; however, it was significantly higher in the P+S+OS column (89.7% in P+S+OS and 70.1% in P+S). To elucidate the methods of removal in each column and to investigate the biofilm growth throughout each column and differences in growth on the different media, SEM-EDS analysis was done at the end of the study. This chapter presents and discusses the investigation of

the use of oyster shells as a biofilm carrier in the Particulate Pyrite Autotrophic Denitrification (PPAD) system.

Table 3.1. Description of column study comparing P+S+OS and P+S adapted from Tong et al. (2017)

Phase	**Length of study (d)**	**HRT**	**Organic C addition?**	**TIN removal efficiency (%)**	
				P+S	P+S+OS
I	10 - start-up 20 - flow through	2.92 h	No	52.4	39.6
II	30 - flow through	2.92 h	No	51.2	35.8
III	30 - flow through	2.92 h	Yes	42.4	43.8
IV	20 – flow through	6 h	Yes	70.1	89.7

3.2 Literature Review

3.2.1 Pyrite Oxidizing Denitrification

Pyrite and other ferrous sulfide minerals have been investigated as alternative electron donor media to elemental sulfur for autotrophic denitrification. Torrento et al. (2010) showed increased denitrification rates in columns inoculated with *Thiobacillus denitrificans* in the presence of pyrite compared with inoculated columns without pyrite and un-inoculated columns with and without pyrite, showing that pyrite can serve as an electron donor for the denitrifying bacteria. Torrentó et al. (2012) studied the attachment and growth of the autotrophic bacterium *Thiobacillus denitrificans* on pyrite surfaces. The results from the study showed that there were more free-living cells in the solution than attached cells; however, both contributed to denitrification. The study indicated that both direct (attached processes for electron donor oxidation) and indirect (electron donor access via solution) processes are important for pyrite oxidizing denitrification. Energy dispersive x-ray spectroscopy (EDS) was used to confirm the

presence of biofilm on pyrite surfaces. Pyrite surfaces that were not covered with biofilm had unchanged carbon and oxygen atomic percentages from before to after the study (32% for C and 8% for O), while those covered with biofilm had higher carbon and oxygen atomic percentages after the study (42-51% for C and 8-13% for O). S and Fe decreased fairly proportionately after the study, with the atomic percentage of Fe showing a slightly higher decrease than S (from 39% to 25-29% and from 21% to 12-13%, respectively).

Pu et al. (2014) evaluated the effectiveness of pyrite-based autotrophic denitrification using acid-treated (AP) and untreated pyrite (UP). Both AP and UP treatment of the synthetic groundwater resulted in good nitrate removal rate constants and sulfate production; however, AP columns had a higher rate constant and lower sulfate production of 1.03 d^{-1} and 224 mg L^{-1} compared to 0.95 d^{-1} and 388 mg L^{-1} for UP columns. The authors also observed a stable pH for both columns, indicating that denitrification using pyrite as an electron donor has another advantage over SOD of not needing an additional alkalinity source.

Li et al. (2016) investigated the effectiveness of a ferrous sulfide mineral called pyrrhotite ($Fe_{1-x}S$) as an electron donor for autotrophic denitrification. Three side by side columns were tested during this study. The first (B1), the control, contained only limestone, the B2 biofilter contained only pyrrhotite, and the B3 column contained a 1:1 volume ratio of pyrrhotite to limestone. Removal efficiencies of NO_3^- and PO_4^{3-} in B3 were as high as 96% and 95%, respectively for synthetic wastewater and Total Nitrogen (TN) and PO_4^{3-} removal efficiencies in real wastewater were 91% and 87%, respectively. The phosphorus in the column formed secondary minerals with the dissolved iron formed during denitrification, so the phosphorus removal was correlated to the denitrification rate. Column B3 also showed the lowest sulfate production of the two columns containing pyrrhotite and lower sulfate concentrations were observed and it was hypothesized that

heterotrophic denitrification was taking place utilizing dead or lysed bacteria within the column as the carbon source. This process did not produce sulfate.

3.2.2 Particulate Pyrite Autotrophic Denitrification

Particulate Pyrite Autotrophic Denitrification (PPAD) is a process which uses particulate pyrite as the electron donor for autotrophic denitrification, sand as a nonreactive biofilm carrier and oyster shell as an alkalinity source. Tong et al. (2017a) compared PPAD to Sulfur Oxidizing Denitrification (SOD) in column studies and saw a lower denitrification efficiency in PPAD (39%) compared to SOD (99%). However, less sulfate production was observed in PPAD (5.66 mg SO_4^{2-}/mg NO_3^--N compared to 7.54 mg SO_4^{2-}/mg NO_3^-- N in SOD) and lower alkalinity consumption of PPAD (1.70 mg $CaCO_3$/mg NO_3^--N compared to 4.57 mg $CaCO_3$/mg NO_3^--N in SOD) show that it is a promising technology. In the same study, Tong et al. (2017a) conducted microcosm experiments comparing PPAD denitrification rates to those of SOD. Denitrification rates of PPAD were found to approach those of SOD (0.86 mg L^{-1} h^{-1} and 1.19 mg L^{-1} h^{-1}, respectively). Denitrification in PPAD is carried out by the following overall reaction, where the iron and sulfur in pyrite is oxidized by chemolithotrophic bacteria and NO_3^- is reduced to form N_2 gas (Torrento et al. 2010):

$$FeS_2 + 3NO_3^- + 2H_2O \rightarrow 2SO_4^{2-} + 1.5N_2 + Fe(OH)_3 + H^+ \quad (6)$$

For each g of NO_3^--N removed during the PPAD process, 4.57 g SO_4^{2-} is produced and 1.7 g of alkalinity (as $CaCO_3$) is consumed (Tong et al., 2017a).

PPAD produced lower sulfate and consumed less alkalinity than the SOD process. Due to the lower alkalinity consumption, further studies by Tong et al. (2017b) compared the performance of PPAD columns with and without oyster shell (P+S+OS and P+S, respectively) to determine if oyster shell has other benefits in the column.

3.2.3 Oyster Shell as a Biofilm Carrier

The high specific surface area of oyster shell makes it a more effective biofilm carrier than other materials. Sengupta et al (2007) used BET analysis to determine the specific surface area of oyster shell (2.37 m^2/g), which is much higher than that of quartz sand (0.85 m^2/g) found by Lai et al. (2000) using the same method. Sengupta et al. (2007) also used SEM-EDS analysis to observe morphology and elemental composition differences between oyster shell, limestone and marble. They found that oyster shell had a much rougher surface, and concluded that the higher surface area and rough morphology of the oyster shell surface made it ideal as a biofilm carrier. Caffrey et al. (2016) demonstrated the nitrification/denitrification capability of attached growth on oyster shells and living oysters in natural systems (estuaries). They found that living oysters and shells had no significant difference in nitrification rates, but that living oysters had a greater denitrification rate (3 times) than shells only. Even so, shells showed a 3.3 times greater denitrification rate than nitrification rate, indicating that they are an effective biofilm carrier for denitrification. Ivanov et al. (2006) observed the growth of ammonia-oxidizing bacteria on the surface of oyster shells in an aquaculture biofiltration system.

3.3 Materials and Methods

3.3.1 Sample Collection

Details of the column set up and operation are given in Tong et al. (2017b). Media samples from after the experiment were hand collected from port 1 (near influent) and port 5 (near effluent) of the P+S and P+S+OS columns. The column with ports is shown in Figure 3.1. At least three of each media type was collected for biofilm imaging. A protein study was done during the study based on methods used by Boles et al. (2012) and biomass was removed from the media based on

methods used by Wang et al. (2014). Samples used for elemental analysis were collected after the protein study, which used a brine solution to remove all biofilm.

Figure 3.1. Image of one column from the experiment with vertical ports labeled.

3.3.2 SEM-EDS

Scanning Electron Microscopy (SEM) was used to observe the distribution of the biofilm on different medium components and at different depths, Ports 1 (near influent) and 5 (near effluent). Scanning Electron Microscopy-Energy-Dispersive X-Ray Spectroscopy (SEM-EDS) was used to observe the changes in medium composition due to microbial leaching by comparing fresh samples with clean (biofilm removed) samples collected at the end of the study. Imaging and EDS analysis was done in duplicate using a Hitachi S800 field emission gun scanning electron microscope (Hitachi, USA).

Samples were prepared for biofilm imaging using a modification of methods described by Torrentó et. al. (2012) and Zhang et. al. (2015). Briefly, media samples were hand separated according to media type, column and position into centrifuge vials from the column after the 110-

day column study by Tong et al. (2017b) described in Table 3.1 above. The samples were initially washed with DI water and then fixed with 2.5% glutaraldehyde in a pH 7.1 phosphate buffer solution at room temperature (20 ± 2 ºC) for 30 min. The samples were then washed with phosphate buffer solution and then gradually dehydrated for 10 minutes each in solutions with concentrations of 25%, 50%, 75%, and 100% ethanol mixed with DI water. Samples were then dried by soaking 2×5 min in 99+% electronic grade hexamethyldisilazane (HMDS) and left to air dry in the fume hood overnight. The phosphate buffer solution was prepared by dissolving 7.9 g NaCl, 0.2 g KCl, 0.24 g KH_2PO_4, 1.8 g K_2HPO_4 in 800 mL distilled water. Fresh and cleaned media samples (after protein analysis) were prepared for SEM-EDS by washing 2×10 seconds in acetone, drying and subsequently coating with gold-palladium (Au-Pd) film.

3.3.3 Statistical Analysis

One-Way Analysis of Variance (ANOVA) was used to calculate the P values (probability) for the EDS results. A P-value with a 95% confidence level was considered significant and a 99% confidence level was considered highly significant.

3.4 Results and Discussion

3.4.1 SEM-EDS Results

EDS results for particulate pyrite and oyster shells before (fresh samples) and after the study are shown in Table 3.2. Significant differences were observed in iron and sulfur of pyrite from the P+S+OS column and carbon from the oyster shell. In samples taken from the influent port (port 1), atomic percentages for S on the pyrite surface increased significantly (α=0.05) from 59.91% ± 0.10% to 62.36% ± 0.11% coupled with a decrease in Fe. In samples taken from the effluent port (port 5), atomic percentages for S on the pyrite surface decreased significantly (α=0.05) from 59.91% ± 0.10% to 53.94% ± 0.37% in P+S+OS column. Significant changes were

not observed in atomic percentages from media collected from the P+S column, however they followed the trends of pyrite Fe and S from the P+S+OS column. Based on Kong et al. (2016) and experimental results indicating low $Fe(OH)_3$ precipitation and low Fe^{3+} complexation in batch studies, Tong et al. (2017b) concluded that the dominant mechanism for denitrification in both columns was pyrite S_2^{2-} oxidation to S^0, SO_3^{2-}, $S_2O_3^{2-}$, and/or SO_4^{2-}. This conclusion was supported by the significant increase in the atomic percentage of Fe and decrease in S for the P+S+OS column effluent during the PPAD process and supports the occurrence of NO_3^- reduction coupled with pyrite oxidization (Torrentó et al., 2010; Tong et al., 2017). In batch biofilm studies, Torrentó et al. (2012) observed a higher decrease in Fe atomic percentage than S when using EDS on the surface of the pyrite with biofilm attached, which is supported by findings from the influent port mentioned above. Bonnissel-Gissinger et al. (1998) observed an accumulation of Fe(III) hydroxides on the pyrite surface during oxidation at neutral pH which could also explain the changes in atomic percentage observed in the effluent.

Carbon atomic percentages in the oyster shells significantly decreased from 45.29% ± 0.38% to 38.39% ± 1.15% in the P+S+OS column effluent, indicating some dissolution due to alkalinity consumption. No significant differences were observed in Ca and O atomic percentages in the oyster shells from before the experiment to the port 5 samples. Atomic percentage changes cannot be used to determine an increase or decrease of a certain component if all measured components are changing, so alkalinity consumption cannot be deduced from this data. However, these results can be explained by the composition of oyster shell. Oyster shell is composed of crystalline phases of $CaCO_3$ held together by an organic scleroprotein compound called conchiolin (Sengupta et al., 2007). In theory, as alkalinity (as $CaCO_3$) is consumed, entire crystals are dissolved, but the conchiolin matrix is also broken up to release the crystals, leading to a

disproportional decrease in the atomic percentage of carbon in relation to calcium and oxygen atomic percentage changes on the oyster shell. Therefore, a decrease in carbon atomic percentage can be used to deduce some alkalinity consumption.

Alkalinity data collected by Tong et al. (2017b) show consistently higher alkalinity from the P+S+OS system compared to the P+S system, showing that dissolution of oyster shells occurred and/or some heterotrophic denitrification could have contributed alkalinity during stages III and IV.

3.4.2 SEM Images to Observe Surface Characteristics and Biofilm Distributions

SEM images are shown in Figure 3.2. Figure 3.2 a, b and c show media surfaces without biofilm. Pyrite, shown in Figure 3.2 a, has a smooth surface compared to sand and oyster shell (Figure 3.2 b and c). Due to this, pyrite showed low biofilm attachment (Figure 3.2 d. f, h and k). which is supported in findings by Torrentó et al. (2012). In normal biofilters, more biofilm growth would be expected in the influent to the column, where substrate concentrations are high. Oyster shell showed the greatest biofilm growth and distribution (Figure 3.2 j) in port 1 (influent) which is supported by the protein in matrix biomass results (Figure 3.3 a). Sand also showed high biofilm growth (Figure 3.2 e, g, i and l). Higher biofilm growth was observed on sand from port 5 (effluent) in both columns (Figure 3.2 g and l). In the column without oyster shell (P+S), greater biofilm growth was observed on the quartz sand compared to that in the P+S+OS column in port 1 (influent), showing that oyster shell is a more preferential surface for biofilm attachment than sand due to its rough surface, as observed in Figure 3.2 c, and in Caffrey et al. (2016). Figure 3.3 a shows protein results from biofilm attached to the media and 3.3 b shows protein from the pore water in the column. Results indicate that the P+S+OS column had higher biofilm attachment than the P+S column near the influent and less near the effluent.

Table 3.2. Energy Dispersive X-Ray Spectroscopy data (averages) in atomic percentage units for pyrite and oyster shell samples from before the experiment and taken from port 1 (near inlet) and port 5 (near outlet) n = 2.

Media		**Before experiment**	**P+S column port 1**	**P+S column port 5**	**P+S+OS column port 1**	**P+S+OS column port 5**
		%				
Pyrite	Fe	40.06 ± 0.10	37.84 ± 0.95	42.39 ± 4.21	37.64 ± 0.11	46.07 ± 0.37
	S	59.91 ± 0.10	62.17 ± 0.95 (p=0.08)	57.61 ± 4.21 (p=0.72)	62.36 ± 0.11 (p=0.002)	53.94 ± 0.37 (p=0.03)
Oyster shells	Ca	17.34 ± 1.13	-	-	18.96 ± 1.02 (p=0.31)	23.41 ± 7.57 (p=0.5)
	C	45.29 ± 0.38	-	-	41.72 ± 1.09 (p=0.06)	38.39 ± 1.15 (p=0.01)
	O	37.37 ± 0.75	-	-	39.25 ± 0.06 (p=0.86)	38.22 ± 6.43 (p=0.87)

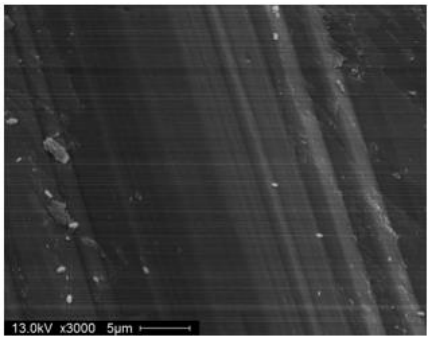

(a) Pyrite before the experiment

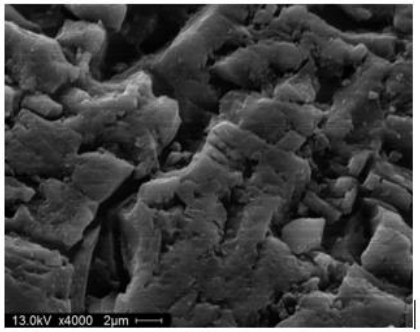

(b) Quartz sand before the experiment

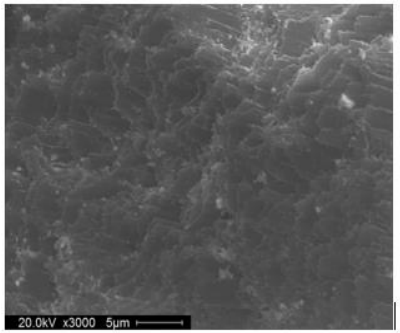

(c) Oyster shell before the experiment

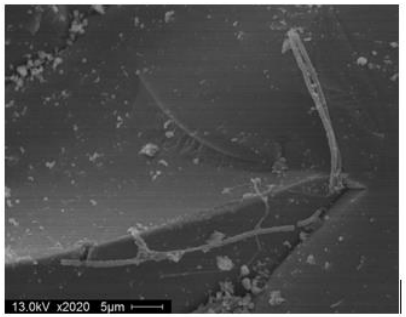

(d) Particulate pyrite in P+S port 1

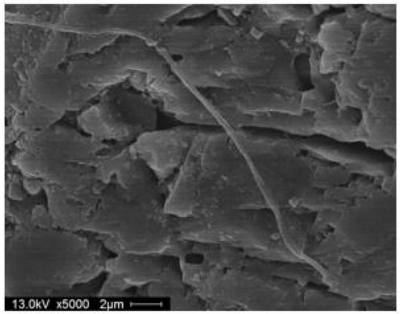

(e) Quartz sand in P+S port 1

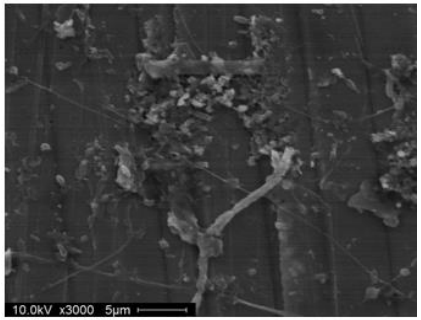

(f) Particulate pyrite in P+S port 5

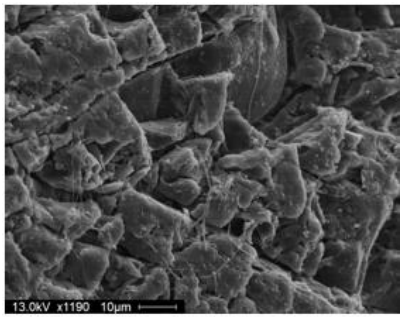

(g) Quartz sand in P+S port 5

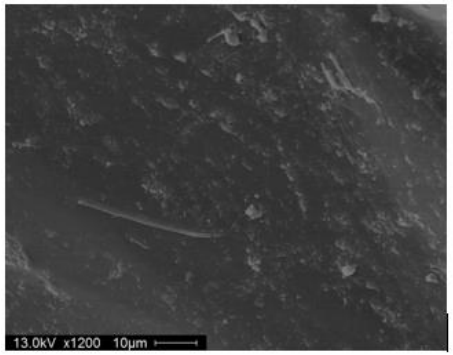

(h) Particulate pyrite in P+S+OS port 1

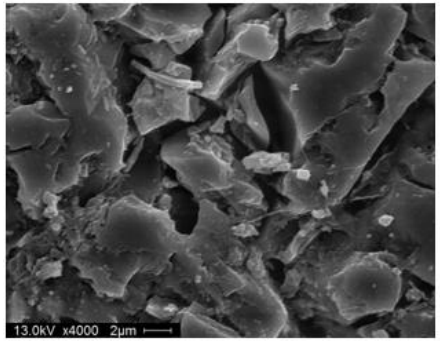

(i) Quartz sand in P+S+OS port 1

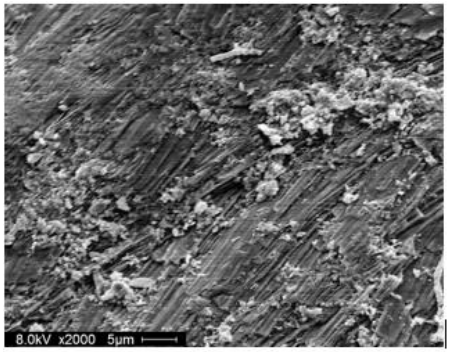

(j) Oyster shell in P+S+OS port 1

Figure 3.2. SEM images of particulate pyrite, quartz sand and oyster shell before (a, b and c) and after the experiment from ports 1 (influent) and 5 (effluent) from the P+ S column (d, e, f and g) and ports 1 and 5 from the P+S+OS column (h, i, j, k, l and m).

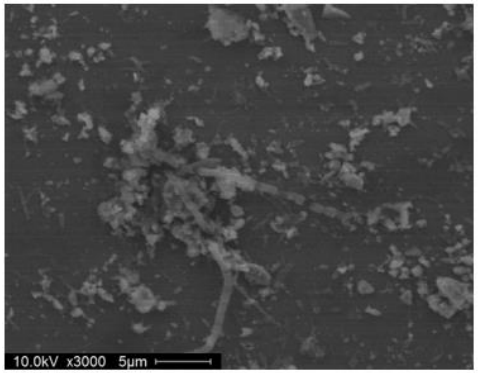

(k) Particulate pyrite in P+S+OS port 5

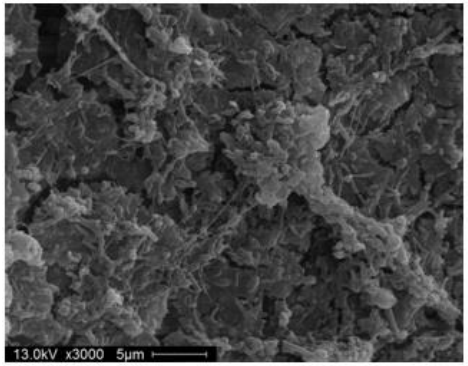

(l) Quartz sand in P+S+OS port 5

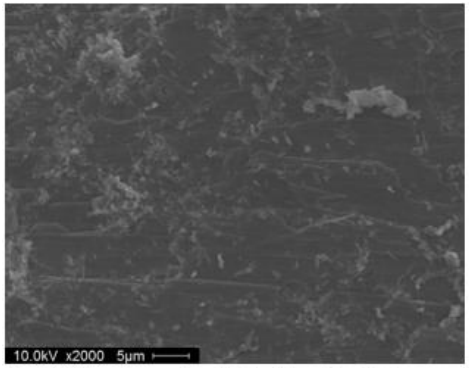

(m) Oyster shell in P+S+OS port 5

Figure 3.2 (Continued)

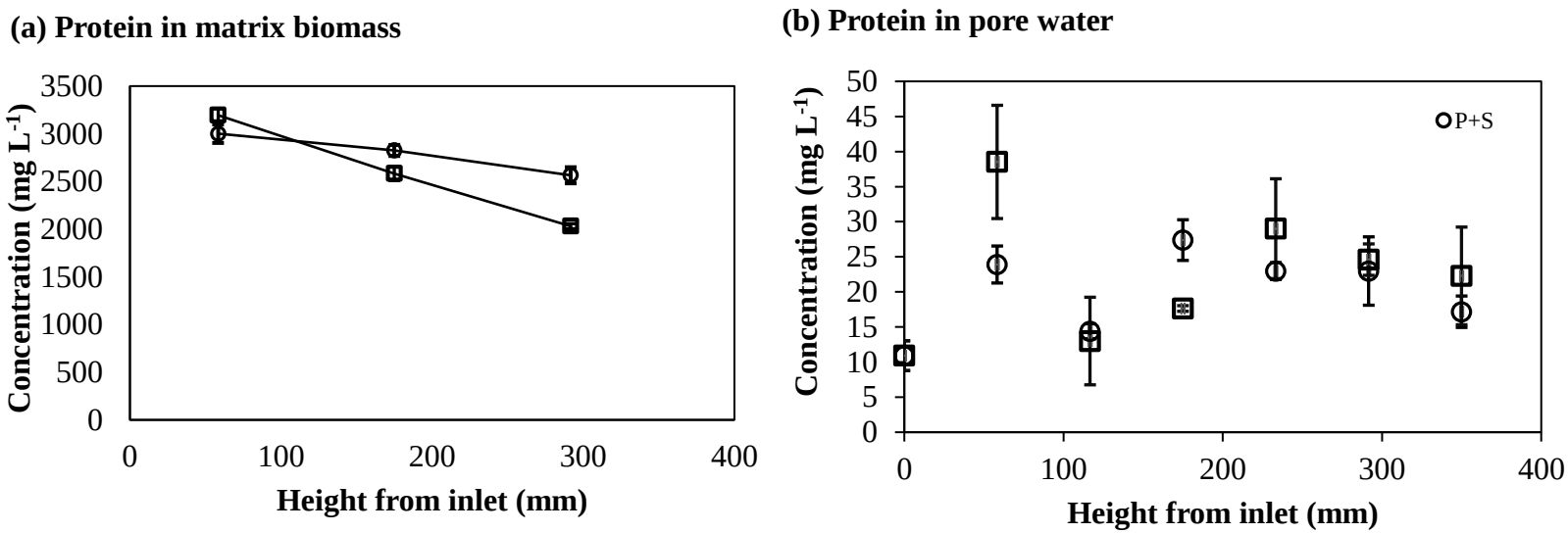

Figure 3.3. Protein results from a) attached biomass and b) pore water from Tong et al. (2017b)

3.5 Conclusions

The objective of this chapter was to investigate the role of oyster shells in pyrite oxidizing denitrification. SEM results indicated that oyster shell is a preferential surface for biofilm attachment, as high biofilm coverage was observed on oyster shell compared to pyrite. In the P+S column, SEM images showed that the sand surface was the preferential surface for biofilm attachment and that the smooth surface of pyrite did not offer a good surface for biofilm attachment. In addition, low attachment to pyrite indicates that biofilm access to substrate occurs mostly in the bulk liquid as opposed to via direct contact with the pyrite surface.

EDS results showed that denitrification was coupled with pyrite oxidation. Changes in the sulfur and iron atomic percentages of pyrite indicate that sulfur is still the main electron donor for denitrification in pyrite oxidation and/or that Fe(III) accumulation is occurring on the pyrite surface, due to low/no detection of Fe (II) or Fe(III) in column effluents.

CHAPTER 4: CONCLUSIONS AND RECOMMENDATIONS

The startup of a pilot scale Hybrid Adsorption and Biological Treatment System (HABiTS) was evaluated in Chapter 2 of this thesis. The startup phase (first 10 days) of the pilot scale system showed the characteristic spike in sodium (Na^+) with a corresponding drop in ammonium (NH_4^+) concentrations from stage 1 of both systems, indicating adsorption of NH_4^+ on the clinoptilolite. After 10 days, a peak in nitrification intermediate product nitrite (NO_2^-) concentrations indicated acclimation of nitrifiers in the filters. NH_4^+ removal in FF-1 was less than that observed by Rodriguez-Gonzalez et al. (2017) in bench scale studies of HABiTS (70% compared to 80%) but the NH_4^+ removal in R-1 exceeded this (87%).

The second objective of the pilot study was the investigation of the effect of nitrification stage 1 recirculation on nitrogen removal in the HABiTS system. TIN removal efficiencies for nitrification stage 1 give a clue into the effect of recirculation on treatment efficiencies. R-1 had a TIN removal efficiency of 35.4% compared to 28.8% in FF-1. Average sCOD concentrations for R-1 and FF-1 were not significantly different, however Biochemical Oxygen Demand (BOD) (which represents the biologically available portion of sCOD) measurements could give a better insight into the extent of pre-denitrification caused by recirculation. Higher nitrification rates in R-1 contributed to higher overall TIN removal in R (88.8%) compared to FF (54.9%).

The third objective of this study was to elucidate the role of oyster shell in nitrogen removal in a Particulate Pyrite Autotrophic Denitrification (PPAD) system. Observations made by Scanning Electron Microscopy (SEM) confirmed that oyster shell has a rough surface and observations of biofilms on sand, pyrite and oyster shell from the column with oyster shell

(P+S+OS) and the column without (P+S) showed that oyster shell is a preferential surface for biofilm attachment and that pyrite's smooth surface offers little surface area for biofilm growth.

Energy dispersive X-Ray Spectroscopy (EDS) was used to compare atomic percentages from the surface of pyrite and oyster shell from before the column study and after to deduce microbial processes and which elements were leached during the study. Significant changes in sulfur (decrease) and iron (increase) from pyrite, especially from port 1 (influent) of the column supported the conclusion that denitrification is coupled with pyrite oxidation and that Fe(III) complexes accumulate on the pyrite surface at neutral pH.

Further evaluation of the HABiTS pilot system will be carried out at the 3:1 nitrification stage 1 effluent recirculation ratio for R-1. Future studies of the HABiTS pilot system will include the evaluation of treatment efficiencies of different stage 1 effluent recirculation ratios. Constant recirculation will also be evaluated in the future. Additional studies may also include a manipulation of denitrification stage 2 media, with the possible addition of expanded clay to offset some of the tire chip portion or replacing the elemental sulfur with pyrite as the solid-phase electron donor. An additional stage will also be added for enhanced disinfection for possible reuse of the final effluent of the system. For implementation in a household, the system with recirculation has the potential to only be operated by 1 pump, which could either be on a timer or gravity switch, and the forward flow can be gravity fed, depending on the depth to water and topography of the site.

Future studies with pyrite oxidation in PPAD will also evaluate denitrification efficiency and by product production at varying pH. Studies evaluating denitrification efficiencies of different iron sulfide minerals, such as pyrrhotite will also be conducted and evaluated by Phreeq C.

REFERENCES

APHA. (2012) Standard methods for the examination of water and wastewater, 21st edition. American Public Health Association/American Water Works Association/Water Environment Federation, Washington, DC, USA.

Ames, L. L. (1960). The Cation Sieve Properties of Clinoptilolite. *The American Mineralogist,* 45, 689-700.

Amini, A., Aponte-Morales, V., Wang, M., Dilbeck, M., Lahav, O., Zhang, Q., Cunningham, J., Ergas, S.J. (2017). Cost-effective treatment of swine wastes through recovery of energy and nutrients. *Waste Management,* 69, 508-517.

Anderson, D., Tyl, M., Otis, R.J., Mayer, T.G., Sherman, K. M. (1998). Onsite Wastewater Nutrient Reduction Systems (OWNRS) For Nutrient Sensitive Environments. Prepared for Florida Department of Health (FDOH).

Aponte-Morales, V. (2015). Ammonium Removal from High Strength Wastewater Using a Hybrid Ion Exchange Biological Process (Doctoral dissertation).

Boles, A.R., Conneely, T., McKeever, R., Nixon, P., Nusslein, K.R., Ergas, S.J. (2012). Performance of a pilot-scale packed bed reactor for perchlorate reduction using a sulfur oxidizing bacterial consortium. *Biotechnology and Bioengineering,* 109, 637-646.

Bonnissel-Gissinger, M.A., Ehrhardt, J.J., Behra, P. (1998). Surface Oxidation of Pyrite as a Function of pH. *Environmental Science &Technology,* 32, 2839-2845.

Bricker, S., Longstaff, B., Dennison, W., Jones, A., Boicourt, K., Wicks, C., Woerner, J. (2007). Effects of nutrient enrichment in the nation's estuaries: a decade of change. NOAA Coastal Ocean Program, Decision Analysis Series No. 26. National Centers for Coastal Ocean Science, Silver Spring, MD

Caffrey, J.M., Hollibaugh, J.T., Mortazavi, B. (2016). Living oysters and their shells as sites of nitrification and denitrification. *Marine Pollution Bulletin,* 112, 86-90.

Costa, J., Heufelder, G., Foss, S., Milham, N., Howes, B. (2002). Nitrogen Removal Efficiencies of Three Alternative Septic System Technologies and a Conventional Septic System. *Environment Cape Cod,* 5, 15-24.

Crittenden, J. C., Trusse., R. R., Hand, D. W., Howe, K. J., Tchobanoglous, G. (2012). Principles of Water Treatment. John Wiley & Sons: Hoboken, New Jersey, USA.

EPA (2017) National Primary Drinking Water Regulations. Retrieved from the United States Environmental Protection Agency website: www.epa.gov

FDOH (2013). Standards for Onsite Sewage Treatment and Disposal Systems, Chapter 64E-6, Florida Administrative Code. Florida Department of Health (FDOH).

FOSNRS. (2015). Florida Onsite Sewage Nitrogen Reduction Strategies Study: Final Report. Retrieved from the Florida Department of Health (FDOH) website: www.floridahealth.gov.

Hazen and Sawyer (2014). FOSNRS Study: PNRS II Test Facility Final Report. Prepared for the Florida Department of Health, Bureau of Onsite Sewage Programs under FDOH-Contract CORCL. Tallahassee, FL.

Hazen and Sawyer (2015). FOSNRS Study: Evaluation of Full-Scale Prototype Passive Nitrogen Reduction Systems (PNRS) and Recommendations for Future Implementation. 2 Volumes. Prepared for the Florida Department of Health, Bureau of Onsite Sewage Programs under FDOH Contract CORCL. Tallahassee, FL.

Hirst, J., Anderson, D., Smith, D. (2015). Performance Evaluation of In-Tank Passive Nitrogen Reduction Systems (PNRS). Proceedings of NOWRA/VOWRA/SORA/NAWT Onsite Wastewater Mega-Conference, Uniting for Progress, Virginia Beach, VA, November 4-6, 2015.

Inyang, M., Gao, B., Yao, Y., Xue, Y., Zimmerman, A. (2012). Removal of heavy metals from aqueous solution by biochars derived from anaerobically digested biomass. *Bioresource Technology*, 110, 50-56.

Ivanov, V., Stabnikova, O., Sihanonth, P., Menasveta, P. (2006). Aggregation of ammonia-oxidizing bacteria in microbial biofilm on oyster shell surface. *World Journal of Microbiology & Biotechnology*, 22:807-812.

Kellough, R.M. (1991). The Effects of Scrap Automobile Tires in Water, p. 52. Ontario.

Kong, Z., Li, L., Feng, C., Dong, S., Chen, N. (2016). Comparative investigation on integrated vertical-flow biofilters applying sulfur-based and pyrite-based autotrophic denitrification for domestic wastewater treatment. *Bioresource Technology*, 211, 125-135.

Koon, J. M. & Kaufman, W. J. (1971). Optimization of ammonia removal by ion exchange using clinoptilolite. University of California, CA (USA).

Krayzelova, L., Lynn, T.J., Banihani, Q., Bartacek, J., Jenicek, P., Ergas, S.J. (2014). A Tire-Sulfur Hybrid Adsorption Denitrification (T-SHAD) process for decentralized wastewater treatment. *Water Research*, 61, 191-199.

Lahav, O. & Green, M. (1997). Ammonium removal using ion exchange and biological regeneration. *Water Resources* 32, 2019-2028.

Lai, C.H., Lo, S.L., Chiang, H.L. (2000). Adsorption/desorption properties of copper ions on the surface of iron-coated sand using BET and EDAX analyses. *Chemosphere,* 41, 1249-1255.

Lapointe, B.E., O'Connell, J.D., Garrett, G.S. (1990). Nutrient couplings between on-site sewage disposal systems, groundwaters, and nearshore surface waters of the Florida Keys. *Biogeochemistry,* 10(3), 289-307.

Lee, J. H., Lee, S. M., Choi, G. C., Park, H. S., Kang, D. H.,Park, J. J., 2011. Microbial community analysis in the autotrophic denitrification process using spent sulfidic caustic by denaturing gradient gel electrophoresis of PCR-amplified genes. *Water Science Technology,* 63, 475-483.

Li, R., Morrison, L., Collins, G., Li, A., Zhan, X. (2016). Simultaneous nitrate and phosphate removal from wastewater lacking organic matter through microbial oxidation of pyrrhotite coupled to nitrate reduction. *Water Research,* 96, 32-41.

Lisi, R. D., Park, J. K., Stier, J.C. (2004). Mitigating nutrient leaching with a sub-surface drainage layer of granulated tires. *Waste Management,* 24, 831-839.

Lopez-Ponnada, E.V., Lynn, T.J., Peterson, M., Ergas, S.J., Mihelcic, J.R. (2017). Application of denitrifying wood chip bioreactors for management of residential non-point sources of nitrogen. *Journal of Biological Engineering,* 11, 16.

Metropolitan St. Louis Sewer District. (2016). Project Clear Sewer Connection and Septic Tank Closure Program

Moon, H.S., Nam, K., Kim, J.Y. (2006). Initial Alkalinity Requirement and Effect of Alkalinity Source in Sulfur-Based Autotrophic Denitrification Barrier System. *Journal of Environmental Engineering,* 132, 971-975.

NSF (2013). NSF/ANSI 40-2013 Residential Wastewater Treatment Systems. NSF International, Ann Arbor, Michigan.

Nelson, S.M., Mueller, G., Hemphill, D.C. (1994). Identification of tire leachate toxicants and a risk assessment of water quality effects using tire reefs in canals. *Bulletin of Environmental Contamination,* 52, 574-581.

Pu, J., Feng, C., Liu, Y., Li, R., Kong, Z., Chen, N., Tong, S., Hao, C., Liu, Y. (2014). Pyrite-based autotrophic denitrification for remediation of nitrate contaminated groundwater. *Bioresource Technology,* 173, 117-123.

Rittmann, B.E., McCarty, P. L. (2001). Environmental Biotechnology : Principles and Applications. McGraw Hill Education (India) Private Limited, New Delhi.

Rodriguez-Gonzalez, L., Payne, K., Trotz, M., Anderson, D., Ergas, S.J. (2015). Hybrid Adsorption and Biological Treatment Systems (HABiTs) for onsite wastewater treatment, Proc. 88th Annual Meeting Water Environment Federation (WEFTEC 15), Chicago, IL, September 26-30, 2015.

Rodriguez-Gonzalez, L. (2017). Advanced Treatment Technologies for Mitigation of Nitrogen and Off-flavor Compounds in Onsite Wastewater Treatment and Recirculating Aquaculture Systems (Doctoral dissertation).

Sahinkaya, E., Dursun, N., Kilic, A., Demirel, S., Uyanik, S., Cinar, O. (2011). Simultaneous heterotrophic and sulfur-oxidizing autotrophic denitrification process for drinking water treatment: control of sulfate production. *Water Resources,* 45, 6661–6667

Sahinkaya, E., Durson, N. (2012). Sulfur-oxidizing autotrophic and mixotrophic denitrification process for drinking water treatment: Elimination of excess sulfate production and alkalinity requirement

Sanchez, O., Aspe, E., Marti, M.C., Roeckel, M. (2004). The Effect of Sodium Chloride on the Two-Step Kinetics of the Nitrifying Process. *Water Environment Federation,* 76. 73-80.

Sengupta, S., Ergas, S.J., Lopez-Luna, E. (2007). Investigation of solid-phase buffers for sulfur-oxidizing autotrophic denitrification. *Water Environment Resources,* 79, 2519-2526.

Shulluck, Tom (1990). A Report on the Use of Shredded Scrap Tires in On-Site Sewage Disposal Systems. *Envirologic, State of Vermont Department of Environmental Conservation.*

Sprynskyy, M., Lebedynets, M., Radoslaw, Z., Namiesnik, J., Boguslaw, B. (2005). Ammonium removal from aqueous solution by natural zeolite, Transcarpathian mordenite, kinetics, equilibrium and column tests. *Separation and Purification Technology,* 14, 155-160.

Tong, S., Rodriguez-Gonzalez, L., Payne, K., Feng, C., Ergas, S. (2017). Comparison of particulate pyrite autotrophic denitrification (PPAD) and sulfur oxidizing denitrification (SOD) for treatment of nitrified wastewater. *Water Science & Technology*, 75, 239-246.

Tong, S., Stocks, J., Rodriguez-Gonzalez, L., Feng, C., Ergas, S. (2017). Effect of oyster shell and organic substrate on the performance of a particulate pyrite autotrophic denitrification (PPAD) process. *Bioresource Technology,* 244, 296-303.

Torrento, C., Cama, J., Urmeneta, J., Otero, N., Soler, A. (2010). Denitrification of groundwater with pyrite and *Thiobacillus denitrificans*. *Chemical Geology,* 278, 80-91.

Torrento, C., Urmeneta, J., Edwards, J., Cama, J. (2012). Characterization of Attachment and Growth of *Thiobacillus denitrificans* on Pyrite Surfaces. *Geomicrobiology Journal*, 29, 379-388.

USEPA (2002). Onsite Wastewater Treatment Systems Manual. EPA 625-R-00-008. United States Environmental Protection Agency (USEPA). Office of Research and Development, Washington D.C, USA.

USEPA (2007). Biological Nutrient Removal Processes and Costs. United States Environmental Protection Agency (USEPA). Office of Water, Washington, DC, USA.

USEPA (2017) National Primary Drinking Water Regulations. United States Environmental Protection Agency (USEPA). Office of Water, Washington, DC, USA.

University of Wisconsin-Madison. (1978). Management of Small Wastewater Flows. EPA600/7-78-173. U.S. Environmental Protection Agency, Office of Research and Development, Municipal Environmental Research Laboratory (MERL) Cincinnati, OH.

Wang, M., Kuo-Dahab, W.C., Dolan, S., Park, C. (2014). Kinetics of nutrient removal and expression of extracellular polymeric substances of the microalgae, *Chlorella* sp. and *Micractinium* sp. in wastewater treatment. *Bioresource Technology,* 154, 131-137.

Wright, R.O., Lewander, W.J., Woolf, A.D. (1999). Methemoglobinemia: Etiology, pharmacology, and clinical management. *Annals of Emerging Medicine,* 34, 646-656.

Xie, B., Dai, X. & Xu, Y. (2006). Enhancement of activated sludge performance on ammonium removal by clinoptilolite. *Toxicological & Environmental Chemistry*, 88, 197-206.

Zhang, L., Zhang, C., Hu, C., Liu, H., Qu, J. (2015). Denitrification of groundwater using a sulfur-oxidizing autotrophic denitrifying anaerobic fluidized-bed MBR: performance and bacterial community structure. *Applied Microbiology and Biotechnology*, 99, 2815-2827.

APPENDIX A LIST OF ACRONYMS

BOD- Biochemical Oxygen Demand

BNR- Biological Nitrogen Removal

sCOD- Soluble Chemical Oxygen Demand

FF- Forward Flow only

FOSNRS- Florida Onsite Sewage Nitrogen Reduction Strategies

HABiTS- Hybrid Adsorption and Biological Treatment Systems

IC- Ion Chromatography

IX- Ion Exchange

MCL- Maximum Contaminant Level

OWTS- Onsite Wastewater Treatment Systems

P+S- Pyrite + Sand

P+S+OS- Pyrite + Sand + Oyster Shell

PNRS- Passive Nitrogen Removal Systems

PPAD- Particulate Pyrite Autotrophic Denitrification

R- Recirculation

SEM-EDS- Scanning Electron Microscopy-Energy Dispersive X-Ray Spectroscopy

SOD- Sulfur Oxidizing Denitrification

STE- Septic Tank Effluent

T-SHAD- Tire-Sulfur Hybrid Adsorption Denitrification

TIN- Total Inorganic Nitrogen

TKN- Total Kjeldahl Nitrogen

TN- Total Nitrogen

TSS/VSS- Total Suspended Solids/Volatile Suspended Solids

USEPA- United States Environmental Protection Agency

APPENDIX B SUPPLEMENTARY DATA FOR CHAPTER 2

The following data was used to calculate average concentrations for table 2.6 from Chapter 2.

Table B.1. Daily water quality data for the influent of R and FF.

Day	Na^+ (mg L^{-1})	NH_4^+-N (mg L^{-1})	K^+ (mg L^{-1})	Ca^{2+} (mg L^{-1})	Mg^{2+} (mg L^{-1})	Cl^- (mg L^{-1})	NO_2^--N (mg L^{-1})	NO_3^--N (mg L^{-1})	PO_4^{3-}-P (mg L^{-1})	SO_4^{2-}-S (mg L^{-1})	TN (mg L^{-1})
2	118.18	40.33	25.24	191.21	40.67	152.36	0.19	0	51.15	3.15	
3	114.08	43.62	23.08	138.01	49.02	153.93	0.19	0	17.84	2.92	
4	108.05	41.80	22.80	131.07	53.25	144.64	0.17	0.02	20.39	2.61	65.33
8	104.10	44.15	19.18	164.00	48.82	125.06	0.23	0	11.51	1.26	
9	101.09	42.90	18.63	155.65	46.67	127.16	0.17	0	11.98	1.44	
10	110.37	44.17	20.58	162.55	46.08	141.72	0.15	0	13.93	4.05	
14	72.16	33.65	13.27	148.38	36.16	115.14	0.13	0	10.30	4.23	
15	57.47	28.00	11.71	146.27	35.24	122.48	0.13	0	14.22	2.56	
16	76.94	36.07	15.36	148.35	41.83	125.44	0.14	0	11.83	6.86	
17	59.42	31.27	13.03	147.40	35.62	122.96	0.17	0	13.75	1.63	57.52
18	99.18	43.20	19.42	154.31	44.65	128.21	0.17	0	12.92	1.56	
21	98.88	42.18	18.70	153.80	41.13	115.32	0.13	0.10	14.18	3.44	
22	102.20	41.38	19.84	158.65	41.36	118.38	0.45	0.02	14.39	4.41	
23	106.77	43.95	20.02	164.51	49.14	123.37	0.46	0	14.03	3.96	
24	108.51	46.22	20.38	161.09	40.91	126.85	0.43	0.02	15.48	4.86	53.51
25	103.54	44.33	19.54	157.52	39.51	125.31	0.65	0.02	14.05	4.85	
28	113.41	44.69	18.59	205.09	48.09	132.58	0.39	0	9.73	6.18	
29	115.88	46.22	19.55	209.53	48.80	135.66	0.44	0	10.12	5.34	
30	113.55	44.37	18.61	173.84	41.08	134.81	0.43	0	11.01	6.89	33.06
31	110.59	43.88	18.01	168.48	39.29	131.94	0.40	0.04	11.93	7.71	

Table B.1 (Continued)

37	108.55	42.74	17.75	166.87	38.21	121.87	0.31	0.08	7.47	10.10	
44	100.89	41.67	16.74	169.46	37.88	115.08	0.47	0.01	5.08	4.78	
45	104.34	41.74	17.33	169.73	38.84	119.47	0.27	0	10.40	5.35	
49	103.08	38.39	17.06	171.76	37.41	117.06	0.76	0	8.70	8.48	
51	99.18	36.05	16.82	164.34	35.37	110.47	0.39	0	8.49	10.51	
52	103.64	36.44	19.45	168.64	37.62	117.11	0.58	0	5.78	11.95	54.11
56	106.65	37.65	18.38	166.91	35.68	118.86	0.58	0.01	9.01	7.91	
58	104.42	36.49	18.80	163.39	36.17	116.75	0.28	0	10.42	10.42	

Table B.2. Daily water quality data for R-1

Day	Na^+ (mg L^{-1})	NH_4^+-N (mg L^{-1})	K^+ (mg L^{-1})	Ca^{2+} (mg L^{-1})	Mg^{2+} (mg L^{-1})	Cl^- (mg L^{-1})	NO_2^--N (mg L^{-1})	NO_3^--N (mg L^{-1})	PO_4^{3-}-P (mg L^{-1})	SO_4^{2-}-S (mg L^{-1})	TN (mg L^{-1})
2	283.81	5.06	17.91	120.64	37.16	157.13	0.18	0.00	47.67	27.74	
3	289.89	4.05	16.80	78.91	34.54	166.10	0.10	0.00	16.88	38.27	
4	276.08	5.14	18.08	81.23	37.33	159.63	0.78	0.36	17.03	28.56	8.04
8	218.57	6.98	21.01	108.02	53.27	144.55	2.19	5.91	12.64	27.34	
9	201.88	5.56	20.70	102.13	49.27	133.06	2.78	8.57	11.05	25.62	
10	186.99	7.07	22.41	113.11	49.03	135.91	7.17	7.47	11.27	23.74	
14	117.13	4.18	15.30	114.43	36.55	140.14	7.92	23.39	11.27	24.45	
15	118.38	5.43	17.75	118.45	34.48	135.54	8.61	15.55	11.49	23.38	
16	116.31	3.75	16.85	111.52	34.81	133.37	8.01	17.60	11.16	23.01	
17	119.84	3.48	18.05	108.30	36.05	131.37	8.60	15.73	10.81	23.79	36.07
18	117.71	3.25	16.91	108.15	37.16	122.62	7.65	17.18	10.77	22.62	
21	149.86	4.18	20.98	116.36	43.31	120.44	5.96	14.11	11.64	21.97	
22	154.09	3.76	21.75	119.43	43.21	123.65	5.99	17.15	11.64	23.53	
23	154.43	3.91	22.35	121.67	42.66	125.83	5.44	20.00	12.58	24.16	
24	153.67	4.86	22.59	123.22	42.94	129.11	5.49	19.49	12.33	24.66	32.26
25	150.89	4.35	22.41	124.73	42.02	126.76	5.24	20.20	12.81	24.94	
28	149.71	5.40	23.53	157.29	49.57	127.78	3.28	25.62	9.59	24.44	
29	142.80	8.18	23.69	165.19	49.67	127.05	3.53	19.96	9.22	21.01	
30	151.57	6.18	24.41	142.84	43.79	136.57	4.40	21.34	10.64	24.42	36.47

Table B.2 (Continued)

31	144.51	5.31	23.75	134.84	40.71	134.38	2.66	26.30	10.44	24.54	
37	132.74	4.58	22.79	132.24	36.15	128.54	0.12	34.46	6.99	25.91	34.66
44	126.53	3.85	22.02	136.41	35.23	121.74	0.88	32.80	8.56	24.58	
45	124.26	3.64	21.90	135.89	34.79	120.40	0.95	32.91	7.60	24.33	
49	114.09	2.86	21.01	134.66	33.44	113.44	0.17	32.08	7.92	22.76	
51	118.46	2.78	22.27	136.07	33.45	116.04	0.11	30.89	7.15	23.08	
52	115.51	6.19	23.94	146.09	34.53	115.33	0.16	21.74	8.29	22.97	39.27
56	112.13	8.62	24.78	152.99	35.08	115.91	0.36	9.20	9.09	25.54	
58	111.67	8.43	24.60	151.22	34.13	114.48	0.12	9.19	9.01	26.93	

Table B.3. Daily water quality data for R-2

Day	Na^+ (mg L^{-1})	NH_4^+-N (mg L^{-1})	K^+ (mg L^{-1})	Ca^{2+} (mg L^{-1})	Mg^{2+} (mg L^{-1})	Cl^- (mg L^{-1})	NO_2^--N (mg L^{-1})	NO_3^--N (mg L^{-1})	PO_4^{3-}-P (mg L^{-1})	SO_4^{2-}-S (mg L^{-1})	TN (mg L^{-1})
2											
3											
4											
8											
9											
10											
14											
15											
16											
17	138.73	8.47	25.22	135.03	38.04	131.54	0.14	0.00	8.29	32.50	5.10
18	96.17	1.21	14.34	111.92	33.36	131.53	0.14	0.00	8.85	30.60	
21	167.93	3.06	23.49	121.79	45.73	133.07	0.08	0.00	11.83	36.06	
22	156.90	2.34	21.93	122.04	43.01	128.98	0.38	0.00	11.82	31.50	
23	159.36	1.66	21.63	131.47	42.80	126.84	0.35	0.00	11.25	20.15	
24	160.37	2.91	22.23	134.05	41.95	129.24	0.33	0.00	12.13	11.98	0.00
25	132.43	2.25	18.65	126.82	38.88	119.26	0.48	0.02	11.12	4.69	
28	152.06	3.34	24.01	174.01	49.50	126.08	0.32	0.00	10.84	6.83	

Table B.3 (Continued)

29	154.61	3.51	24.17	180.80	50.36	132.85	0.31	0.00	11.24	6.61	
30	147.56	4.43	23.21	151.31	44.41	127.90	0.32	0.00	9.82	8.12	7.15
31	147.25	4.66	23.33	149.64	41.23	133.84	0.34	0.00	10.86	6.83	
37	136.67	3.77	23.38	157.24	43.31	129.50	0.27	0.00	5.86	11.05	5.63
44	127.58	2.81	22.55	166.52	33.97	131.04	0.22	0.00	7.64	9.54	
45	118.63	1.90	20.95	157.85	34.44	113.77	0.29	0.00	7.03	13.54	
49	126.76	1.93	23.35	153.51	34.62	121.93	0.47	0.02	7.11	17.51	
51	118.02	2.65	22.51	161.12	35.58	119.29	0.39	0.00	7.75	20.71	
52	116.53	4.03	22.45	149.85	33.09	116.66	0.52	0.00	7.74	28.96	9.04
56	108.54	7.90	23.82	152.78	34.81	111.12	0.61	0.03	10.66	24.75	
58	109.96	9.13	24.24	149.83	33.48	112.38	0.39	0.00	7.54	32.44	

Table B.4. Daily water quality data for FF-1

Day	Na^+ (mg L^{-1})	NH_4^+-N (mg L^{-1})	K^+ (mg L^{-1})	Ca^{2+} (mg L^{-1})	Mg^{2+} (mg L^{-1})	Cl^- (mg L^{-1})	NO_2^--N (mg L^{-1})	NO_3^--N (mg L^{-1})	PO_4^{3-}-P (mg L^{-1})	SO_4^{2-}-S (mg L^{-1})	TN (mg L^{-1})
2	264.97	6.19	16.49	97.36	32.92	156.33	0.13	0.37	17.61	20.35	
3	291.85	2.34	14.91	75.16	32.89	159.45	0.25	0.37	15.08	24.55	
4	270.68	5.20	16.41	78.36	39.91	150.46	0.54	0.88	15.31	19.56	9.28
8	209.51	10.33	20.64	110.86	53.18	140.57	2.92	4.64	11.16	24.98	
9	197.04	11.30	23.39	113.01	51.05	134.72	3.81	6.76	10.39	22.73	
10	179.67	13.00	23.33	120.88	50.08	137.48	4.71	9.26	10.96	22.97	
14	108.48	11.08	18.41	130.84	38.20	138.54	3.80	12.54	11.17	23.31	
15	97.96	7.24	15.72	118.80	34.87	132.10	3.76	14.37	11.33	23.70	
16	132.34	9.51	21.16	119.08	37.97	129.29	3.39	15.74	10.82	24.41	
17	104.09	8.64	19.60	122.30	36.48	131.16	3.55	15.70	10.80	24.57	28.85
18	122.22	11.92	22.41	121.72	39.22	124.49	3.39	13.96	11.57	23.94	
21	152.05	13.93	27.37	135.21	45.32	131.91	3.12	14.58	11.76	27.24	
22	138.13	12.49	25.40	132.45	42.00	119.22	2.47	14.48	11.16	24.30	

Table B.4 (Continued)

23	144.98	9.98	26.41	154.99	42.50	121.92	2.81	9.53	11.89	19.42	
24	145.93	17.42	27.31	140.29	41.89	124.47	2.48	8.26	12.33	18.94	31.90
25	123.29	13.70	24.56	136.47	38.21	114.36	0.39	15.13	10.76	23.73	
28	140.25	16.22	27.60	177.73	48.60	135.54	1.26	18.43	10.44	26.11	
29	146.83	17.99	25.77	184.35	48.95	132.65	2.34	10.06	9.95	18.95	
30	141.14	17.45	26.63	160.14	42.00	141.18	0.22	17.13	9.59	27.82	36.47
31	134.44	18.59	26.69	155.18	40.77	137.16	0.25	16.40	10.25	23.38	
37	131.17	14.07	26.23	146.36	36.33	132.72	0.61	26.28	8.44	27.16	38.27
44	119.64	12.75	24.63	151.09	35.21	119.96	0.91	22.17	7.56	23.29	
45	118.05	13.06	24.99	151.75	35.16	118.71	1.01	22.41	7.99	20.55	
49	115.08	10.30	24.84	147.84	34.24	119.99	0.24	29.14	7.30	23.88	
51	112.29	11.21	24.48	147.20	33.65	112.65	0.10	21.73	7.67	21.24	
52	114.05	13.41	24.90	153.89	34.86	118.42	0.21	18.72	9.30	23.71	35.26
56	112.10	14.34	24.42	155.76	33.80	117.02	0.37	13.02	8.54	27.74	
58	107.08	14.15	24.42	151.91	33.15	111.52	0.07	14.40	8.38	29.15	

Table B.5. Daily water quality data for FF-2

Day	Na^+ (mg L^{-1})	NH_4^+-N (mg L^{-1})	K^+ (mg L^{-1})	Ca^{2+} (mg L^{-1})	Mg^{2+} (mg L^{-1})	Cl^- (mg L^{-1})	NO_2^--N (mg L^{-1})	NO_3^--N (mg L^{-1})	PO_4^{3-}-P (mg L^{-1})	SO_4^{2-}-S (mg L^{-1})	TN (mg L^{-1})
2											
3											
4											
8											
9											
10											
14											
15											
16											

Table B.5 (Continued)

17	88.12	6.52	17.63	127.80	32.29	130.99	0.15	0.00	7.64	32.39	11.57
18	130.93	9.56	22.17	123.53	38.50	120.55	0.14	0.00	8.52	29.04	
21	144.25	11.81	25.88	139.66	45.82	126.35	0.11	0.00	11.89	5.67	
22	143.64	11.02	25.52	146.39	43.97	124.10	0.38	0.00	11.18	4.60	
23	144.98	9.98	26.41	154.99	42.50	125.44	0.38	0.00	10.93	8.08	
24	136.14	11.75	26.29	161.29	39.95	123.24	0.36	0.02	10.56	9.70	17.48
25	138.28	12.49	26.65	163.93	38.46	122.42	0.53	0.00	11.19	15.87	
28	130.86	14.28	26.17	203.24	45.02	123.42	0.35	0.00	10.28	16.22	
29	136.13	14.11	26.80	205.45	45.24	128.58	0.34	0.00	9.07	20.77	
30	141.36	15.11	26.69	175.99	40.66	136.38	0.36	0.00	9.43	17.08	19.13
31	134.41	14.02	25.97	173.75	38.72	135.47	0.36	0.00	10.20	18.46	
37	131.20	11.97	26.98	164.23	40.18	121.57	0.24	0.00	3.86	19.83	19.73
44	121.39	10.05	25.13	184.77	33.48	124.58	0.31	0.00	6.97	18.82	
45	119.14	10.76	24.83	176.73	35.64	119.08	0.26	0.00	8.10	18.65	
49	117.37	13.52	25.40	166.23	38.30	121.06	0.74	0.02	8.51	10.93	
51	115.89	13.33	24.99	158.67	36.66	115.26	0.47	0.00	7.74	17.22	
52	115.77	15.76	25.17	155.05	35.42	117.07	0.44	0.00	8.70	22.75	18.14
56	112.07	14.94	24.42	155.81	33.89	114.05	0.43	0.00	7.84	35.72	
58	106.83	14.66	23.58	152.45	32.70	110.05	0.37	0.00	9.19	32.82	

APPENDIX C DESIGN SPECIFICATIONS AND PHOTOS OF THE PILOT SYSTEM

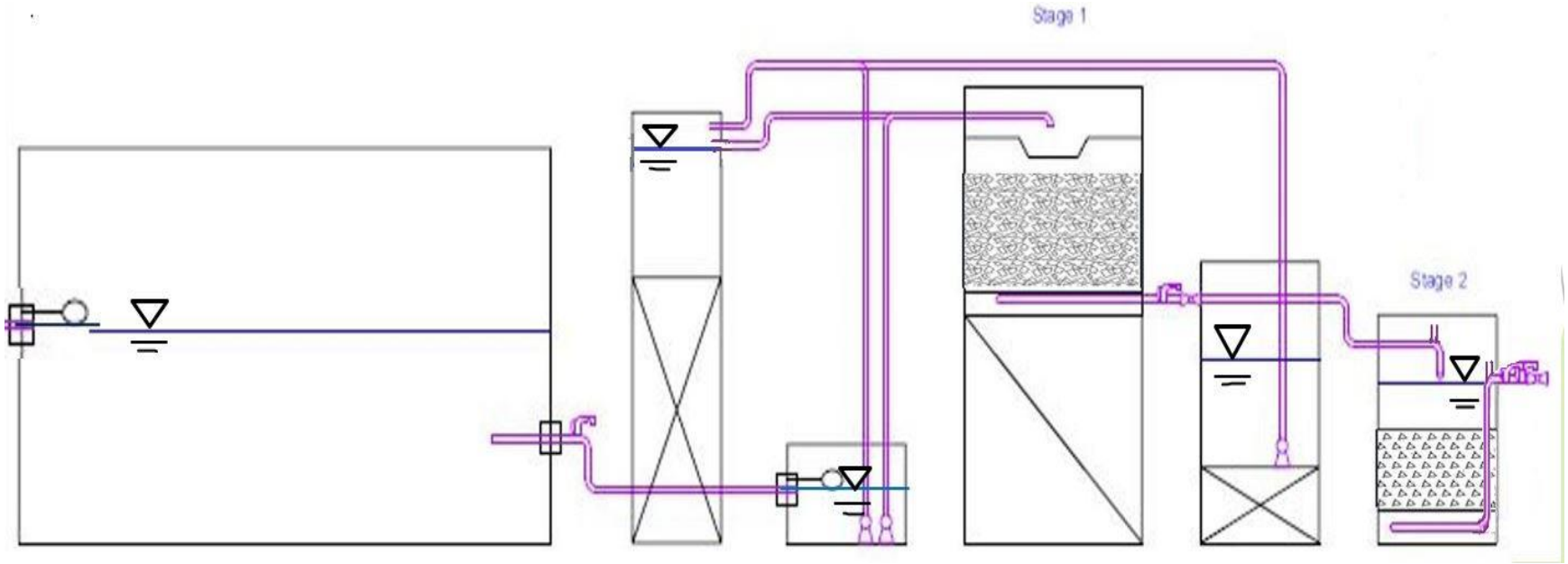

Figure C.1. Complete sketch of pilot system from recirculation (R) side. Not drawn to scale.

Figure C.2. Image taken from the forward flow (FF) side of the pilot system, showing (left to right) stage 2, stage 1 and the septic tank.

Figure C.3. Image taken of the R side of the pilot system showing (left to right) stage 2, recirculation pump tank, stage 1, and recirculation tank.

APPENDIX D COPYRIGHT PERMISSION

Portions of the work presented in Chapter 3 (Figure 3.2 and Figure 3.3) have been previously published in the journal *Bioresource Technology*. The figures were cited where appropriate.

Journal author rights

In order for Elsevier to publish and disseminate research articles, we need publishing rights. This is determined by a publishing agreement between the author and Elsevier. This agreement deals with the transfer or license of the copyright to Elsevier and authors retain significant rights to use and share their own published articles. Elsevier supports the need for authors to share, disseminate and maximize the impact of their research and these rights, in Elsevier proprietary journals* are defined below:

For subscription articles	For open access articles
Authors transfer copyright to the publisher as part of a journal publishing agreement, but have the right to: • Share their article for Personal Use, Internal Institutional Use and Scholarly Sharing purposes, with a DOI link to the version of record on ScienceDirect (and with the Creative Commons CC-BY-NC- ND license for author manuscript versions) • Retain patent, trademark and other intellectual property rights (including research data). • Proper attribution and credit for the published work.	Authors sign an exclusive license agreement, where authors have copyright but license exclusive rights in their article to the publisher**. In this case authors have the right to: • Share their article in the same ways permitted to third parties under the relevant user license (together with Personal Use rights) so long as it contains a CrossMark logo, the end user license, and a DOI link to the version of record on ScienceDirect. • Retain patent, trademark and other intellectual property rights (including research data). • Proper attribution and credit for the published work.

***Please note that society or third party owned journals may have different publishing agreements. Please see the journal's guide for authors for journal specific copyright information.**